

What do non-relativistic CFTs tell us about Lifshitz spacetimes?

Cynthia Keeler, Gino Knodel and James T. Liu

*Michigan Center for Theoretical Physics, Randall Laboratory of Physics,
The University of Michigan, Ann Arbor, MI 48109–1040, USA*

E-mail: keelerc@umich.edu, gknodel@umich.edu, jimliu@umich.edu

ABSTRACT: We study the reconstructability of $(d+2)$ -dimensional bulk spacetime from $(d+1)$ -dimensional boundary data, particularly concentrating on backgrounds which break $(d+1)$ -dimensional Lorentz invariance. For a large class of such spacetimes, there exist null geodesics which do not reach the boundary. Therefore classically we expect some information is trapped in the bulk and thus invisible at the boundary. We show that this classical intuition correctly predicts the quantum situation: whenever there are null geodesics which do not reach the boundary, there are also “trapped scalar modes” whose boundary imprint is exponentially suppressed. We use these modes to show that no smearing function exists for pure Lifshitz spacetime, nor for any flow which includes a Lifshitz region. Indeed, for any (planar) spacetime which breaks $(d+1)$ -dimensional Lorentz invariance at any radius, we show that local boundary data cannot reconstruct complete local bulk data.

Contents

1	Introduction	1
2	The Classical Picture: Bulk reconstruction via light signals	4
2.1	Lifshitz geodesics	6
3	The Quantum Picture: Bulk reconstruction for scalar fields	8
3.1	Scalars in Lifshitz spacetime	9
3.2	A Specific Example: $z = 2$ Lifshitz	12
3.3	WKB Approximation	14
4	Smearing Functions in Lifshitz spacetimes	15
4.1	Momentum-space analysis	19
4.2	No smearing function \Leftrightarrow singularities?	20
4.3	Other flows involving Lifshitz	25
5	Generalization	26
5.1	Removing trapped modes via deformations	27
5.2	Adding trapped modes via deformations	28
5.3	Relativistic domain wall flows	29
6	Modifying the bulk-boundary dictionary	29
7	Conclusion	31
A	WKB approximation	33
A.1	Example: AdS ($z = 1$)	36
A.2	Example: $z = 2$ Lifshitz	36
A.3	General Lifshitz	39
A.4	Error analysis	40

1 Introduction

For the past several years, there has been much interest in applying the powerful field theory/gravity dualities developed in the late 90s and early 2000s to field theories without Lorentz invariance. These non-relativistic forms of AdS/CFT, often collectively referred to as AdS/CMT due to their relevance for condensed matter systems, have provided a new tool for examining strongly coupled non-relativistic systems (see, e.g. [1–4] and references therein).

Although many aspects of the bulk-boundary dictionary familiar from AdS/CFT carry forward to these systems without alteration, some aspects differ strongly. The first obvious difference is the symmetry group; since the goal is to consider spacetime duals to nonrelativistic systems, the asymptotic symmetries of the spacetime should be nonrelativistic. As a consequence, the spatial and temporal components of the metric near the boundary must scale differently with the radius. This different scaling in fact means the notion of a boundary itself is altered; using the Penrose definition of a conformal boundary leads to a degenerate boundary metric. However, more careful treatments have shown that there is still a reasonable notion of a boundary as the location where metric components go to infinity, and holographic calculations can be performed using suitable prescriptions [5–11].

The spacetimes studied as possible nonrelativistic duals fall into two main classes: those which have Lifshitz scaling symmetry, and those which have the larger Schrödinger symmetry. There are also other spacetimes in the literature, including the warped AdS spacetimes [12–16], which exhibit temporo-spatial anisotropy. In this paper, we will concentrate on spacetimes which have Lifshitz symmetry at least in some region, but many of our conclusions apply to more general spacetimes with scaling differences between space and time.

One of the best studied examples of a boundary-bulk duality system with space/time anisotropy is the so-called Lifshitz spacetime, given by

$$ds_{d+2}^2 = - \left(\frac{L}{r} \right)^{2z} dt^2 + \left(\frac{L}{r} \right)^2 (d\vec{x}_d^2 + dr^2). \quad (1.1)$$

It was first proposed in [17] and has been extensively studied since. In order to remove some of the concerns about degenerate boundary behavior, [18–20] have considered replacing the near-boundary UV region of the spacetime with an asymptotically AdS spacetime. Other numerical constructions of these backgrounds are available in [21–24]. Additionally, there are a set of “hyperscaling-violating” solutions which still have a Lifshitz-like symmetry, proposed in [25] and studied further in [26–29]. We will consider an ansatz which allows for analysis of all these cases.

Much recent progress has been made in creating a complete bulk/boundary dictionary for nonrelativistic systems [5, 6, 8, 10]. In the well studied case of Lorentzian AdS/CFT, an important part of this dictionary is the correspondence between normalizable modes, which scale as r^{Δ_+} near the boundary, and states in the Hilbert space of the dual field theory. In particular, a quantized bulk field ϕ can be mapped to its corresponding boundary operator O via

$$\phi \mapsto O = \lim_{r \rightarrow 0} r^{-\Delta_+} \phi. \quad (1.2)$$

The remarkable fact here is that both operators can be quantized in terms of the same creation/annihilation operators, which implies an isomorphism between the Fock space representations of bulk and boundary Hilbert spaces [30, 31]. Moreover, the map (1.2) can be inverted in position space. As a result, local quantum fields in the bulk can be expressed in terms of boundary operators with the help of a so-called smearing function K [32–34]. Consequently, we can study CFTs to learn something about their gravitational duals [35–37].

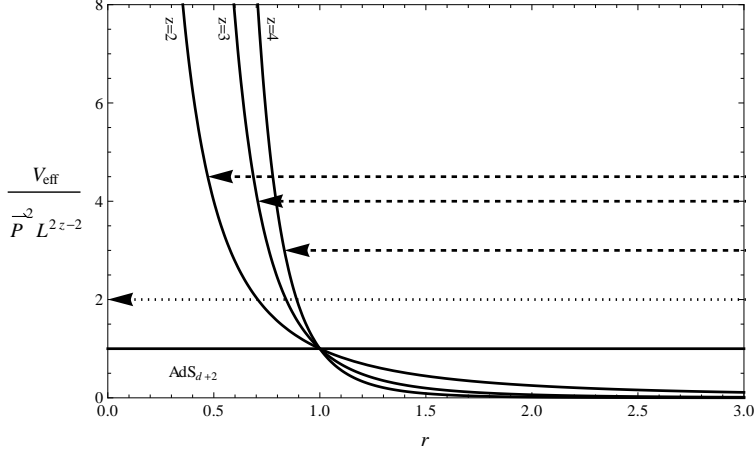


Figure 1. Effective potential (1.3) for null geodesics ($\kappa = 0$) in AdS ($z = 1$) and Lifshitz spacetimes ($z = 2, 3, 4$). In Lifshitz, light rays sent from the bulk in any nonradial direction have to turn around at finite r and can never reach the boundary.

If AdS/CMT is to be understood as a ‘true’ equivalence between a field theory and a gravitational theory, rather than just a set of prescriptions to compute condensed matter quantities, one should expect that a similar statement can be made for nonrelativistic systems. In other words, the field theory should somehow contain all the relevant information about the gravitational theory. In this paper, we address this issue by investigating the extent of the reconstructability of bulk information from boundary data in nonrelativistic spacetimes.

A simple argument why this procedure is not straightforward can be made by studying geodesics in the corresponding backgrounds. For Lifshitz spacetime, the effective potential is given by

$$V_{\text{eff}}(r) = \left(\frac{L}{r}\right)^{2z} \kappa + \left(\frac{L}{r}\right)^{2(z-1)} \vec{p}^2. \quad (1.3)$$

Null geodesics ($\kappa = 0$) with nonzero transverse momentum p turn around at finite r and never reach the boundary (see Figures 1 and 3). This is a result of the nonrelativistic nature of the dual theory, which manifests itself in the fact that the effective speed of light g_{tt}/g_{xx} diverges as $r \rightarrow 0$. Therefore, information about the transverse direction of the bulk geometry can never reach an observer at the boundary.

Quantum mechanically the picture is different. In general, wavefunctions are allowed to tunnel through any classically forbidden region to reach the boundary, so there is hope that bulk reconstruction is possible after all. However, as we will demonstrate, at large momenta the imprint these tunneling modes leave at the boundary is exponentially small and as a consequence, a smearing function cannot be constructed. Our arguments closely follow those of [38, 39], where first steps towards generalizing smearing functions to spaces other than pure AdS were made.

Our analysis for the case of pure Lifshitz spacetime can be easily generalized to show

that smearing functions do not exist for any geometry that allows for ‘trapped modes’, that is, modes that have to tunnel through a momentum-barrier in the potential to reach the boundary. In [39], the authors show that the smearing function in their spherically symmetric spacetimes can indeed become well-defined, at least in some bulk region, once they change from an AdS-Schwarzschild solution to a nonsingular asymptotically AdS spacetime. Our case, however, does not allow such a resolution. Importantly, the smearing function in Lifshitz remains ill-defined everywhere if we resolve the tidal singularity [17, 40, 41] into an $\text{AdS}_2 \times \mathbb{R}^d$ or AdS_{d+2} region. It also remains ill-defined everywhere if we replace the near-boundary region with an asymptotic AdS_{d+2} region, or if we do both replacements at once [21–23].

The problem we encounter when trying to construct a smearing function is related to modes with large transverse momentum. Introducing a momentum-cutoff Λ , however, will force us to give up the ability of reconstructing full bulk locality in the transverse direction.

The outline of this paper is as follows: In section 2, we discuss the idea of bulk reconstruction via classical geodesics in Lifshitz spacetimes. We show that there are null geodesics that cannot reach the boundary. We generalize this statement to flows involving Lifshitz regions, as well as more general nonrelativistic spacetimes with planar symmetry, considering the constraints arising from the null energy condition. In section 3, we turn to the quantum picture and study solutions of the scalar field equations for the same class of spacetimes. In particular, we show analytically that for $z = 2$ Lifshitz, there are modes that have to tunnel through a momentum-barrier in the potential to reach the boundary and are thus exponentially suppressed. We generalize this result to arbitrary z using the WKB approximation. In section 4, we review the construction of smearing functions via the mode-sum approach and attempt to construct a Lifshitz smearing function. Using WKB methods, we show that this attempt fails due to the existence of ‘trapped modes’, which have exponentially small boundary imprint. In section 5, we generalize our findings to show that smearing functions do not exist for a large class of nonrelativistic spacetimes. Finally, in section 6 we interpret our results and their implications for bulk locality. We argue that only a hard momentum cutoff allows bulk reconstruction, at the cost of giving up locality in the transverse direction.

2 The Classical Picture: Bulk reconstruction via light signals

We now set our notation and discuss the classical paths of geodesics within the spacetimes we study. Specifically, we consider planar metrics of the form

$$ds_{d+2}^2 = -e^{2A(r)} dt^2 + e^{2B(r)} d\vec{x}_d^2 + e^{2C(r)} dr^2. \quad (2.1)$$

This ansatz is sufficiently general to include AdS, Lifshitz with general z (with or without hyperscaling violation), $\text{AdS}_2 \times \mathbb{R}^d$ and spacetimes which interpolate among them. Note that one of the three functions A, B and C can always be eliminated by a suitable gauge choice. However, it is convenient to keep these functions arbitrary for now, so that we can more easily accommodate the various gauge choices that have been used for AdS and Lifshitz metrics in

the literature. The metric (2.1) can be trivially rewritten as

$$ds_{d+2}^2 = e^{2B(r)}[-e^{2W(r)}dt^2 + d\vec{x}_d^2] + e^{2C(r)}dr^2. \quad (2.2)$$

where we defined $W \equiv A - B$. For $W = 0$, the $(d+1)$ -dimensional metric at constant r is Lorentz invariant. This encompasses the pure AdS case as well as Lorentz invariant domain wall flows. The $W \neq 0$ case allows for ‘non-relativistic’ backgrounds such as pure or asymptotic Lifshitz backgrounds as well as for planar black holes. In this case, we may interpret e^{-W} as the gravitational redshift factor¹.

The global behavior of the metric is constrained by the null energy condition (subsequently NEC; for previous work see [42, 43]). The two independent conditions are

$$-R_t^t + R_r^r = de^{W-C}\partial_r(-e^{-W-C}\partial_r B) \geq 0, \quad (2.3)$$

$$-R_t^t + R_{x_1}^{x_1} = e^{-W-(d+1)B-C}\partial_r(e^{W+(d+1)B-C}\partial_r W) \geq 0. \quad (2.4)$$

Here x_1 is any one of the \vec{x} transverse directions. If we choose a gauge where $A = C$, or equivalently $W = C - B$, these conditions simplify to

$$((e^{-B})'e^{-2W})' \geq 0, \quad (2.5)$$

$$(W'e^{dB})' \geq 0, \quad (2.6)$$

where $'$ denotes derivatives with respect to the radial coordinate ρ in the corresponding gauge. Since $e^{dB} \geq 0$, we can use the second condition to deduce the following statements about W (see Figure 2):

$$\begin{aligned} \text{If } W'|_{\rho_-} \leq 0 &\Rightarrow W'|_{\rho \leq \rho_-} \leq 0; \\ \text{If } W'|_{\rho_+} \geq 0 &\Rightarrow W'|_{\rho \geq \rho_+} \geq 0. \end{aligned} \quad (2.7)$$

From (2.5) we can deduce similar equations for e^{-B} . If we combine the two constraints (2.5) and (2.6), we learn about the second derivatives of W and e^{-B} when their first derivatives have the same sign:

$$\begin{aligned} \text{If } W'|_{\rho_-} \leq 0 \text{ and } (e^{-B})'|_{\rho_-} \leq 0, &\Rightarrow W''|_{\rho \leq \rho_-} \geq 0 \text{ and } (e^{-B})''|_{\rho \leq \rho_-} \geq 0; \\ \text{If } W'|_{\rho_+} \geq 0 \text{ and } (e^{-B})'|_{\rho_+} \geq 0, &\Rightarrow W''|_{\rho \geq \rho_+} \geq 0 \text{ and } (e^{-B})''|_{\rho \geq \rho_+} \geq 0. \end{aligned} \quad (2.8)$$

These conditions will constrain the bulk geometry, and in particular the behavior of the redshift factor e^{-W} .

As mentioned in the introduction, we may gain insight about the bulk spacetime by considering null geodesics. Such geodesics are easily obtained by noting that the metric (2.1) admits Killing vectors

$$\frac{\partial}{\partial t}, \quad \frac{\partial}{\partial x^i}. \quad (2.9)$$

¹Note that this assumes that there is an asymptotic reference region where $W = 0$, so that $(d+1)$ -dimensional Lorentz invariance is restored. This would occur, for example, in an AdS to Lifshitz flow.

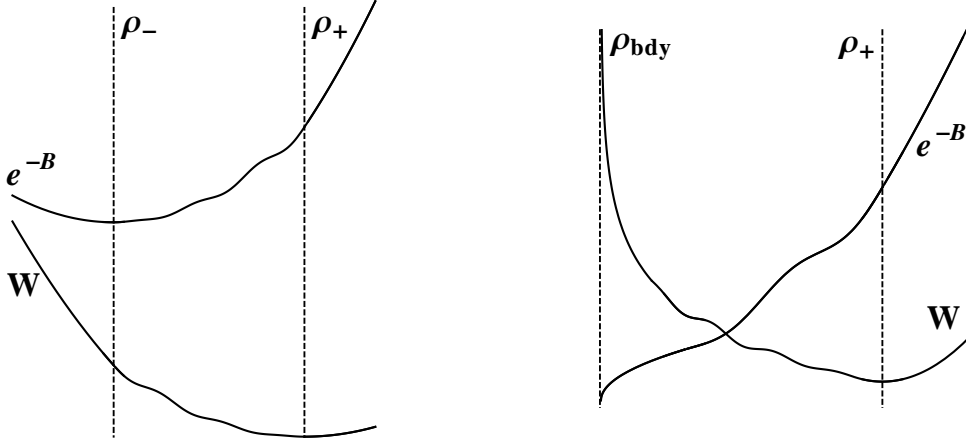


Figure 2. Two sketches of functions W and e^{-B} which obey the null energy conditions (2.5) and (2.6). The figure on the right approaches Lifshitz asymptotics at ρ_{bdy} .

This allows us to define the conserved energy and momentum

$$E \equiv e^{2A}\dot{t}, \quad \vec{p} \equiv e^{2B}\dot{\vec{x}}, \quad (2.10)$$

where a dot indicates a derivative with respect to the affine parameter λ . Geodesics then obey

$$-\kappa = \left(\frac{ds}{d\lambda}\right)^2 = -e^{-2(W+B)}E^2 + e^{-2B}\vec{p}^2 + e^{2C}\dot{r}^2. \quad (2.11)$$

If we define

$$V_{\text{eff}} \equiv e^{2(W+B)}\kappa + e^{2W}\vec{p}^2, \quad (2.12)$$

with $\kappa = 1$ for timelike and $\kappa = 0$ for null geodesics, then we find

$$e^{2(W+B+C)}\dot{r}^2 = E^2 - V_{\text{eff}}. \quad (2.13)$$

This is of the form of an energy conservation equation, $E_{\text{tot}} = E_{\text{kin}} + V_{\text{eff}}$, where

$$E_{\text{kin}} = e^{2(W+B+C)}\dot{r}^2. \quad (2.14)$$

2.1 Lifshitz geodesics

We now study specifically Lifshitz spacetimes. Pure Lifshitz spacetime corresponds to taking

$$W = -(z-1)\log(r/L), \quad B = -\log(r/L), \quad C = -\log(r/L) \quad (2.15)$$

in the metric ansatz (2.2). Note that the ‘horizon’ is at $r = \infty$, while the boundary is at $r = 0$. The effective potential for geodesics is

$$V_{\text{eff}}(r) = \left(\frac{L}{r}\right)^{2z}\kappa + \left(\frac{L}{r}\right)^{2(z-1)}\vec{p}^2. \quad (2.16)$$

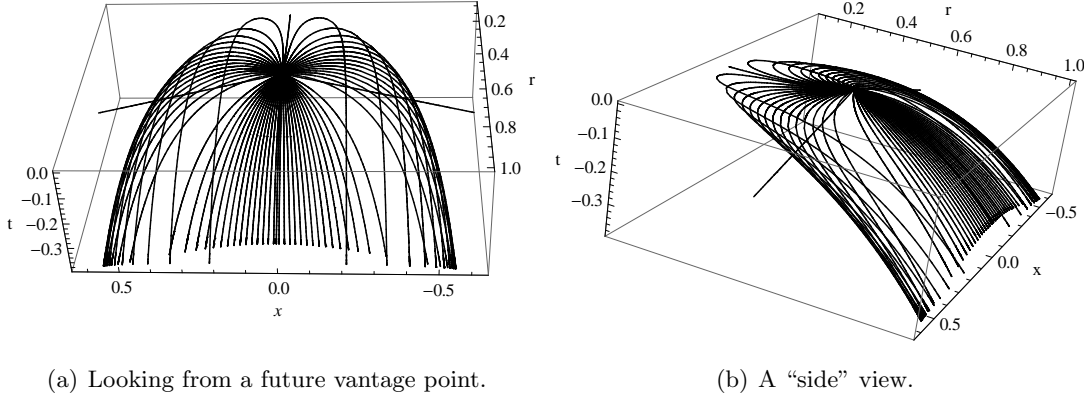


Figure 3. Plot of null curves through the point $t = 0$, $\vec{x} = 0$, $r = 1/2$ in Lifshitz space with $z = 3$.

The behavior of the second term depends on the value of z . For $z = 1$, this term is a constant, and just shifts the overall potential. For $z > 1$, the second term still grows as $r^{-2(z-1)}$, but this growth is slower than that of the κ term. In addition, it vanishes at the horizon, $r \rightarrow \infty$. For null geodesics ($\kappa = 0$), the effective potential is completely determined by this term.

Radial null geodesics ($\vec{p} = 0$) do not feel any effective potential. For $z > 1$, non-radial geodesics on the other hand cannot reach the boundary. In Figure 3, we have plotted several such light rays which all converge on one point in space; these rays delineate the causal past of that point. As we can see in the figure, only the null geodesic which stays at constant $x = 0$ can reach the boundary at $r = 0$; all others turn around at some minimum r .

The result is that a full classical² reconstruction of the bulk from the boundary is not possible. An observer at the boundary can never receive any signals from the bulk which travel with a nonzero momentum in the transverse direction. Consequently, this observer will not be able to ‘resolve’ transverse length scales in the bulk. Of course, this picture is somewhat naive and cannot be taken as a proof that bulk reconstruction is impossible. However, as we will show in the next section, the picture carries forward to the quantum case, even though tunneling through classically forbidden regions is possible.

Two comments are in order at this point. First, notice that pure Lifshitz spacetime has a pathology at $r \rightarrow \infty$. An infalling extended object experiences infinitely strong tidal forces. To see this, consider two parallel radial geodesics with energy E travelling in the background (2.2). The geodesic deviation equation for the transverse separation X^i reads

$$\frac{D^2 X^i}{Dt^2} = X^i E^2 e^{-2(W+B+C)} \left[-B' (W' + C') + B'' - \frac{\kappa}{E^2} e^{2(W+B)} (B' (B' - C') + B'') \right]. \quad (2.17)$$

For Lifshitz spacetime, we have

$$\frac{D^2 X^i}{Dt^2} = X^i \frac{E^2}{L^2} \left[(1 - z) \left(\frac{r}{L} \right)^{2z} - \frac{\kappa}{E^2} \right]. \quad (2.18)$$

²Note that ‘classical’ in this case refers to the geometric optics limit, as opposed to just the $N \rightarrow \infty$ limit.

For $z \neq 1$, the relative acceleration diverges near the horizon and the result is an infinitely strong tidal force. By now, there are several known ways to resolve this issue [21–23, 44]. For solutions which involve a running dilaton, a natural resolution is to avoid the singularity by deforming the geometry such that it flows to $\text{AdS}_2 \times \mathbb{R}^d$ in the deep infrared. More generally, one can imagine several possible IR deformations that change the behavior of the metric functions W , B and C at large r . These deformations have to be consistent with the NECs in (2.5) and (2.6) above. However, it is clear that while these procedures might cure the problems encountered near the horizon, they do not change the fact that geodesics sent towards the boundary still cannot overcome the Lifshitz barrier (2.16).

On the other hand, one could imagine that deforming the geometry in the UV might help null geodesics to reach the boundary. Deformations which replace the UV with an AdS region have the benefit of clarifying the holographic prescription³. If we imagine a geometry that is approximately Lifshitz at some ρ_- , then $W'(\rho_-) < 0$. The NECs thus dictate that e^W has to either continue increasing or asymptote to a constant as $\rho \rightarrow 0$. The latter case would correspond to an AdS to Lifshitz flow. For fixed transverse momentum p , geodesics with large enough energy can now escape the potential and reach the boundary. However, at fixed E , the height of the potential barrier is controlled by p^2 , so geodesics with large transverse momentum remain trapped inside the bulk.

We conclude that for any spacetime that is approximately Lifshitz in some region, part of the information about the bulk will always be hidden from a classical boundary observer. The part that is missing describes physics at large p , or equivalently small transverse length scales. Again, we will see in the subsequent sections that this statement has an exact equivalent in the quantum case.

3 The Quantum Picture: Bulk reconstruction for scalar fields

While the geometric optics picture of the previous section already captures some important physical properties of nonrelativistic gauge/gravity dualities, a full analysis of the problem of bulk reconstruction from the boundary clearly requires a treatment of quantum operators. To this end, we consider solutions to the scalar field equations and investigate what kind of imprint they can leave at the boundary. Specifically, we examine the amplitude of scalar modes near the UV boundary in terms of the size of fluctuations deep in the IR.

We begin by studying the Klein-Gordon equation for a scalar in the fixed background (2.2)

$$[e^{-W-(d+1)B-C} \partial_M e^{W+(d+1)B+C} g^{MN} \partial_N - m^2] \phi = 0. \quad (3.1)$$

Because of the Killing vectors (2.9) present in our metric ansatz, the wave equation is separable and we can write

$$\phi(t, \vec{x}, r) = e^{i(\vec{p} \cdot \vec{x} - Et)} f(r). \quad (3.2)$$

³See, however [5–10] for different approaches to holography in Lifshitz spacetimes.

Then the Klein-Gordon equation (3.1) becomes

$$\left[e^{2(W+B-C)} \left(\partial_r^2 + \frac{d(W + (d+1)B - C)}{dr} \partial_r \right) + E^2 - e^{2W} \vec{p}^2 - e^{2(W+B)} m^2 \right] f = 0. \quad (3.3)$$

Let us choose a gauge where $A = C$, or $W = C - B$. Equivalently, starting in any given gauge we can introduce a new radial coordinate ρ such that

$$e^{C-B-W} dr = d\rho. \quad (3.4)$$

Note that ρ is a tortoise coordinate for our metric ansatz. This gives

$$[\partial_\rho^2 + dB' \partial_\rho + E^2 - e^{2W} \vec{p}^2 - e^{2(W+B)} m^2] f = 0, \quad (3.5)$$

where primes denote derivatives with respect to ρ . If we now let

$$f = e^{-dB/2} \psi, \quad (3.6)$$

we end up with a Schrödinger-type equation

$$-\psi'' + U\psi = E^2\psi, \quad (3.7)$$

where

$$U = V_m + V_p + V_{\text{cos}}, \quad (3.8)$$

with

$$V_m = e^{2(W+B)} m^2, \quad V_p = e^{2W} \vec{p}^2, \quad V_{\text{cos}} = (d/2)B'' + (d/2)^2 B'^2. \quad (3.9)$$

Here V_m and V_p together form the effective potential (2.12) for geodesics, with κ replaced by m^2 . The third term, V_{cos} , is an additional ‘cosmological’ potential that is absent in the classical picture.

3.1 Scalars in Lifshitz spacetime

For Lifshitz backgrounds, the Schrödinger potential can be written as

$$U = \left(\frac{L}{z\rho} \right)^2 \left(m^2 + \frac{d(d+2z)}{4L^2} \right) + \left(\frac{L}{z\rho} \right)^{2(1-1/z)} \vec{p}^2, \quad (3.10)$$

where we introduced a new radial coordinate according to (3.4). Explicitly, we have

$$\rho = \frac{L}{z} \left(\frac{r}{L} \right)^z. \quad (3.11)$$

Note that both V_m and the entirety of V_{cos} contribute to the $1/\rho^2$ blowup as $\rho \rightarrow 0$ (corresponding to the boundary). The fact that these two pieces scale with the same power of ρ is a feature of Lifshitz spacetime; it will not continue to be true for more complicated spacetimes such as the AdS-Lifshitz flows studied in section 4.2.

The qualitative behavior of solutions to the Schrödinger equation is roughly as follows: The wavefunction starts out oscillating deep in the bulk ($\rho \rightarrow \infty$) and crosses the potential barrier at the classical turning point ρ_0 . For $\rho < \rho_0$, the mode must tunnel under the barrier, and thus the wavefunction will in general be a superposition of exponentially growing and suppressed modes. We will only be interested in the mass ranges where the growing solution is non-normalizable. Thus, the normalizable modes relevant for canonical quantization are exponentially suppressed in the area of this barrier at small ρ .

For $z = 1$, V_p is a constant, but for $z > 1$ it blows up near the boundary, although less fast than the other terms in the potential. Specifically, $V_p/V_m \propto e^{-2B}$. For spacetimes with Lifshitz asymptotics,

$$\partial_\rho (e^{-B}) \Big|_{\rho_{\text{bdy}}} = \partial_\rho \left(\frac{z\rho}{L} \right)^{1/z} \Big|_{\rho_{\text{bdy}}} > 0. \quad (3.12)$$

Consequently, $\partial_\rho e^{-B} > 0$ throughout the spacetime. Near the boundary, the mass term V_m will always dominate, but V_p will increase in relative importance as we head in towards the IR region.

Because of the different behavior of the mass/cosmological and momentum-dependent terms, it is crucial to distinguish between two qualitatively different ‘types’ of tunneling. If at a given energy, the momentum \vec{p} is sufficiently small, the wavefunction crosses the barrier at a point where V_p is subdominant compared to the other terms in the potential. Consequently, the $1/\rho^2$ part of U will control the suppression near the boundary. We shall refer to those modes as *free modes*. This name is justified, because even though they are tunneling, classically they correspond to null geodesics that can reach the boundary.

If \vec{p} is large, the wavefunction crosses the barrier already at a point where $U \approx V_p$, and the wavefunction will receive an additional suppression by an exponential in \vec{p} , due to tunneling through this thicker barrier. We shall refer to this class of solutions as *trapped modes*. They play a crucial role in our analysis, as they are the quantum equivalent to nonradial null-geodesics that cannot reach the boundary.

We may study the behavior of these free and trapped modes by solving the Schrödinger equation (3.7) in a Lifshitz background. It is convenient to scale out the energy E by introducing the dimensionless coordinate

$$\zeta = E\rho. \quad (3.13)$$

Then (3.7) becomes $-\psi''(\zeta) + (U - 1)\psi(\zeta) = 0$ where

$$U = \frac{\nu_z^2 - 1/4}{\zeta^2} + \frac{\alpha}{\zeta^k}, \quad (3.14)$$

with

$$\nu_z = \frac{1}{z} \sqrt{(mL)^2 + (d+z)^2/4}, \quad \alpha = \left(\frac{EL}{z} \right)^k \left(\frac{\vec{p}}{E} \right)^2, \quad k = 2(1 - 1/z). \quad (3.15)$$

Since the null energy condition demands $z \geq 1$, we generally focus on the case $0 < k < 2$. (The $k = 0$, or pure AdS, case is familiar and can be treated by standard methods.) In this

case, the boundary ($\zeta \rightarrow 0$) behavior of U is $\sim 1/\zeta^2$, while the horizon ($\zeta \rightarrow \infty$) behavior is $\sim 1/\zeta^k$.

Near the boundary, we have

$$-\psi'' + \frac{\nu^2 - 1/4}{\zeta^2} \psi \approx 0 \quad \Rightarrow \quad \psi \sim A\zeta^{1/2-\nu} + B\zeta^{1/2+\nu}. \quad (3.16)$$

Using (3.11), (3.13) and (3.6), we can express the behavior of the original Klein-Gordon field in terms of the original coordinate r as

$$\phi \sim \hat{A} \left(\frac{r}{L} \right)^{\Delta_-} + \hat{B} \left(\frac{r}{L} \right)^{\Delta_+}, \quad (3.17)$$

where

$$\hat{A} = A \left(\frac{EL}{z} \right)^{1/2-\nu}, \quad \hat{B} = B \left(\frac{EL}{z} \right)^{1/2+\nu}, \quad \Delta_{\pm} = \frac{d+z}{2} \pm \sqrt{(mL)^2 + \left(\frac{d+z}{2} \right)^2}. \quad (3.18)$$

We will consider only the mass range where the first solution (related to A) is non-normalizable with respect to the Klein-Gordon norm, while the second solution (related to B) is normalizable. Via the AdS/CFT correspondence, non-normalizable modes represent classical sources of an operator O at the boundary, which redefine the Hamiltonian of the field theory [45–47]. Normalizable fluctuations are placed on top of these classical sources and they correspond to different states in the field theory, or equivalently expectation values of O [30, 31].⁴ We will only be interested in the situation where the boundary Hamiltonian is fixed, so we will consequently treat non-normalizable solutions as non-fluctuating. The fluctuating modes to be quantized are thus the normalizable modes given by B . As a result, we will end up setting $A = 0$ and investigating the consequences of doing so⁵.

Turning now to the horizon, we see that both terms in (3.14) fall off as $\zeta \rightarrow \infty$. Hence the horizon behavior is given by⁶

$$-\psi'' - \psi \approx 0 \quad \Rightarrow \quad \psi \sim ae^{i\zeta} + be^{-i\zeta}. \quad (3.19)$$

In terms of the original r coordinate, this becomes

$$\psi \sim a \exp \left(i \frac{EL}{z} \left(\frac{r}{L} \right)^z \right) + b \exp \left(-i \frac{EL}{z} \left(\frac{r}{L} \right)^z \right), \quad (3.20)$$

⁴Lifshitz spacetimes present some subtleties when considering alternate quantizations. The range of masses for which both boundary conditions are normalizable is larger than in the AdS case, but modes which would not be normalizable in AdS (but apparently are in Lifshitz) suffer from a novel instability. Particularly in these cases it appears more difficult to redefine the Hamiltonian in the usual way [48–50].

⁵Note that this is in contrast with the computation of AdS/CFT correlators, where B is interpreted as the response to turning on a source A .

⁶For simplicity, we have assumed $1 < k < 2$. For $0 < k \leq 1$, the horizon falloff $\sim 1/\zeta^k$ is insufficiently fast, and the potential becomes long-ranged. This introduces a correction to the horizon behavior of the wavefunction. However, this is unimportant for our discussion, as we have no need for the asymptotic phase of ψ in the classically allowed region.

so that

$$\phi \sim a \left(\frac{r}{L}\right)^{d/2} \exp\left(i \frac{EL}{z} \left(\frac{r}{L}\right)^z\right) + b \left(\frac{r}{L}\right)^{d/2} \exp\left(-i \frac{EL}{z} \left(\frac{r}{L}\right)^z\right). \quad (3.21)$$

The horizon modes correspond to infalling and outgoing waves, given by a and b , respectively. Since the wave equation is second order and linear, the boundary data (A, B) must be linearly related to the horizon data (a, b) . AdS/CFT correlators are generally computed by taking infalling conditions at the horizon, corresponding to $b = 0$, while bulk normalizable modes are given instead by taking $A = 0$ at the boundary. Of course, the precise relation between boundary and horizon data can only be obtained by solving the wave equation. While this cannot be performed in general, the exact solution is known for $z = 2$, where the potential U is analytic. We now turn to this case, as it provides a clean example of the behavior of trapped modes and in particular the exponential suppression that they receive when tunneling under the barrier in the potential.

3.2 A Specific Example: $z = 2$ Lifshitz

For a pure Lifshitz background with $z = 2$, or $k = 1$, the potential (3.14) is analytic in ζ and the Schrödinger equation takes the form

$$-\psi'' + \left(\frac{\nu^2 - 1/4}{\zeta^2} + \frac{\alpha}{\zeta} - 1\right) \psi = 0, \quad (3.22)$$

where $\alpha = \bar{p}^2 L / 2E$. As this is essentially Whittaker's equation, the solution can be written in terms of the Whittaker functions $M_{-i\alpha/2, \nu}(-2i\zeta)$ and $W_{-i\alpha/2, \nu}(-2i\zeta)$, or equivalently in terms of confluent hypergeometric functions [17]. Expanding for $\zeta \rightarrow 0$ and demanding that ψ satisfies the boundary asymptotics (3.16) for normalizable and nonnormalizable modes gives

$$\begin{aligned} \psi = & \left[\left(\frac{i}{2}\right)^{\frac{1}{2}+\nu} B - \left(\frac{i}{2}\right)^{\frac{1}{2}-\nu} \frac{\Gamma(-2\nu)\Gamma(\frac{1}{2}+\nu+\frac{i\alpha}{2})}{\Gamma(2\nu)\Gamma(\frac{1}{2}-\nu+\frac{i\alpha}{2})} A \right] M_{-i\alpha/2, \nu}(-2i\zeta) \\ & + \left[\left(\frac{i}{2}\right)^{\frac{1}{2}-\nu} \frac{\Gamma(\frac{1}{2}+\nu+\frac{i\alpha}{2})}{\Gamma(2\nu)} A \right] W_{-i\alpha/2, \nu}(-2i\zeta). \end{aligned} \quad (3.23)$$

For the horizon, we expand for large ζ and compare with (3.19) to obtain

$$\begin{aligned} \psi = & \left[e^{-\pi\alpha/4} \frac{\Gamma(\frac{1}{2}+\nu+\frac{i\alpha}{2})}{\Gamma(1+2\nu)} 2^{-i\alpha/2} b \right] M_{-i\alpha/2, \nu}(-2i\zeta) \\ & + \left[e^{\pi\alpha/4} 2^{i\alpha/2} a + e^{i\pi(\frac{1}{2}-\nu)} e^{\pi\alpha/4} \frac{\Gamma(\frac{1}{2}+\nu+\frac{i\alpha}{2})}{\Gamma(\frac{1}{2}+\nu-\frac{i\alpha}{2})} 2^{-i\alpha/2} b \right] W_{-i\alpha/2, \nu}(-2i\zeta). \end{aligned} \quad (3.24)$$

Comparing (3.23) with (3.24) gives the relation between horizon and boundary coefficients

$$\begin{aligned} A = & (2i)^{\frac{1}{2}-\nu} \frac{\Gamma(2\nu)}{\Gamma(\frac{1}{2}+\nu-\frac{i\alpha}{2})} e^{\pi\alpha/4} \left(2^{-i\alpha/2} b - e^{i\pi(\frac{1}{2}+\nu)} \frac{\Gamma(\frac{1}{2}+\nu-\frac{i\alpha}{2})}{\Gamma(\frac{1}{2}+\nu+\frac{i\alpha}{2})} 2^{i\alpha/2} a \right), \\ B = & (2i)^{\frac{1}{2}+\nu} \frac{\Gamma(-2\nu)}{\Gamma(\frac{1}{2}-\nu-\frac{i\alpha}{2})} e^{\pi\alpha/4} \left(2^{-i\alpha/2} b - e^{i\pi(\frac{1}{2}-\nu)} \frac{\Gamma(\frac{1}{2}-\nu-\frac{i\alpha}{2})}{\Gamma(\frac{1}{2}-\nu+\frac{i\alpha}{2})} 2^{i\alpha/2} a \right). \end{aligned} \quad (3.25)$$

Although we are primarily interested in normalizable modes in the Lifshitz bulk, we first note that the usual computation of the retarded Green's function proceeds by taking infalling boundary conditions at the horizon, namely $b = 0$. Then (3.24) immediately gives

$$\psi_{\text{infalling}} \sim W_{-i\alpha/2, \nu}(-2i\zeta). \quad (3.26)$$

We now demand that the coefficient of $M_{-i\alpha/2, \nu}(-2i\zeta)$ in (3.23) vanishes, from which we obtain

$$G_R(E, \vec{p}) \sim \frac{\hat{B}}{\hat{A}} = \left(\frac{EL}{2}\right)^{2\nu} \frac{B}{A} = \left(\frac{EL}{i}\right)^{2\nu} \frac{\Gamma(-2\nu)\Gamma(\frac{1}{2} + \nu + \frac{i\alpha}{2})}{\Gamma(2\nu)\Gamma(\frac{1}{2} - \nu + \frac{i\alpha}{2})}, \quad (3.27)$$

in agreement with [17] when continued to Euclidean space. Note that in the large momentum limit, $p \rightarrow \infty$ (or more precisely for $\alpha \gg \nu$), the Whittaker function $W_{-i\alpha/2, \nu}(-2i\zeta)$ is only large near the boundary, and decays exponentially into the bulk. This matches with the heuristic picture of AdS/CFT, where the CFT ‘lives’ on the boundary. In the relativistic case, corresponding to an AdS geometry, the boundary data has a power law falloff as it penetrates into the bulk. However, for this Lifshitz geometry, the falloff is exponential.

Of course, for the bulk reconstruction that we are interested in, we actually want to consider the space of normalizable modes, as they are the ones that span the Hilbert space in the bulk. From the Hamiltonian picture, the natural norm is the Klein-Gordon norm, which is in fact compatible with the norm for the Schrödinger equation (3.7). Normalizable modes correspond to taking $A = 0$, so that

$$\psi_{\text{normalizable}} \sim M_{-i\alpha/2, \nu}(-2i\zeta). \quad (3.28)$$

Comparing (3.23) with (3.24) then gives the relation between bulk and boundary coefficients for normalizable modes

$$\frac{B}{b} = 2^{-i\alpha/2} \left(\frac{2}{i}\right)^{\frac{1}{2} + \nu} \frac{\Gamma(\frac{1}{2} + \nu + \frac{i\alpha}{2})}{\Gamma(1 + 2\nu)} e^{-\pi\alpha/4}. \quad (3.29)$$

Note that $M_{-i\alpha/2, \nu}(-2i\zeta)$ is essentially a standing wave solution in the classically allowed region $\zeta > \zeta_0$, where ζ_0 is the classical turning point. Since this interval is semi-infinite, the wavefunction must be normalized by fixing the amplitude b of these oscillations. Hence the ratio B/b is a direct measure of the amplitude of properly normalized wavefunctions at the boundary.

Recall our previous distinction between the two different types of tunneling solutions: ‘free’ vs. ‘trapped’ modes. Modes with small momenta p at fixed E ($\alpha \ll \nu$) are ‘free modes’. For these modes, we have, up to an overall phase

$$\frac{|B|}{|b|} \approx \frac{2^{\nu + \frac{1}{2}} \Gamma(\frac{1}{2} + \nu)}{\Gamma(1 + 2\nu)}. \quad (3.30)$$

The tunneling process produces the typical scaling behavior $\sim \rho^{\Delta+}$ at the boundary, but there is no exponential suppression. For large momenta ($\alpha \gg \nu$) the modes are ‘trapped’,

and we find instead

$$\frac{|B|}{|b|} \approx \frac{\sqrt{4\pi} e^{-(\nu+\frac{1}{2})}}{\Gamma(1+2\nu)} \alpha^\nu e^{-\pi\alpha/2}. \quad (3.31)$$

These modes have to tunnel not only through the $1/\rho^2$ potential near the boundary, but also through the wider momentum barrier $V_p \sim p^2/\rho$ at larger ρ . This causes the solution to be exponentially suppressed when it reaches the boundary. We conclude that the $z = 2$ Lifshitz metric allows for ‘trapped modes’, which have arbitrarily small boundary imprint for large p .

Clearly, we could have obtained the exponential suppression factor $e^{-\pi\alpha/2}$ in (3.31) by simply setting $V_m = V_{\text{cos}} = 0$ in the Schrödinger potential. More generally, since the size of V_p is controlled by p^2 , in any interval $[\rho_1, \rho_2]$ away from the boundary, i.e. in any region where the potential U is bounded, at large enough p the difference in amplitudes between the points ρ_1 and ρ_2 will always be governed by an exponential relation like (3.31). For the purpose of determining whether or not trapped modes exist in a given spacetime, it will therefore be enough to study the equivalent tunneling problem in the potential $U \equiv V_p$. We will come back to this issue later.

3.3 WKB Approximation

In order to study the existence of trapped modes in spacetimes beyond exact $z = 2$ Lifshitz, it will be useful to have a formalism that provides a qualitative description of the behavior of tunneling modes even for cases where an analytic solution might not exist. This will allow us to study Lifshitz with $z \neq 2$, as well as more general backgrounds (2.2) with nontrivial W , B and C . The WKB method provides us with just such a formalism. We make the standard ansatz

$$\psi \sim \frac{1}{\sqrt{P(\rho)}} e^{\int d\rho' P(\rho')}. \quad (3.32)$$

For slowly-varying potentials, we can plug this back into (3.7) and solve perturbatively for P . The details of this calculation can be found in appendix A. To lowest order, $P^2 \approx U - E^2$ and the solution interpolates between an oscillating region in the bulk and a tunneling region near the boundary. More explicitly, we have

$$\psi(\zeta) = \begin{cases} (U - E^2)^{-\frac{1}{4}} [C e^{S(\rho)} + D e^{-S(\rho)}], & \rho < \rho_0; \\ (E^2 - U)^{-\frac{1}{4}} [a e^{i\Phi(\rho)} + b e^{-i\Phi(\rho)}], & \rho > \rho_0, \end{cases} \quad (3.33)$$

where ρ_0 is the classical turning point and we defined the action $S(\rho) = \int_{\rho}^{\rho_0} d\rho' \sqrt{U - E^2}$ and a phase $\Phi(\rho) = \int_{\rho_0}^{\rho} d\rho' \sqrt{E^2 - U}$. For potentials that behave as $U \sim 1/\rho^2$ near the boundary (which includes both asymptotically AdS and Lifshitz spacetimes), one has to include an additional correction term $U \rightarrow U + 1/(2\rho)^2$ (See appendix A for more details). Using the WKB matching procedure between the two asymptotic regions, we find

$$\begin{aligned} C &= \left(e^{-i\frac{\pi}{4}} a + e^{i\frac{\pi}{4}} b \right), \\ D &= \frac{i}{2} \left(e^{-i\frac{\pi}{4}} a - e^{i\frac{\pi}{4}} b \right). \end{aligned} \quad (3.34)$$

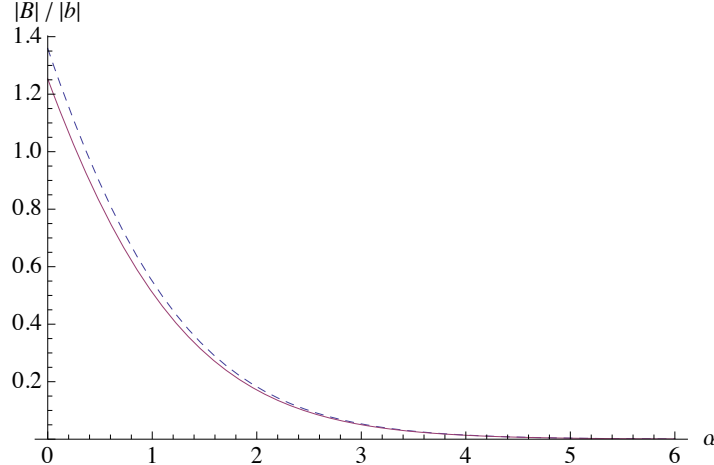


Figure 4. Plot of the WKB (dashed) and exact (solid) boundary normalization factor $|B|/|b|$ as a function of α . Here we have taken $z = 2$ and $\nu = 1$. The large α behavior is exponentially suppressed, $|B|/|b| \sim \alpha^\nu e^{-\pi\alpha/2}$.

The exponential growth/decay of the solution in the classically forbidden region is manifest in the dependence on S in (3.33), which roughly corresponds to the area of the tunneling barrier. The wider/higher the barrier, the larger the corresponding factor e^S is. We are only interested in the normalizable, or decaying solution near the boundary, so we will have to set $C = 0$. Up to a finite error, the WKB approximation then accurately captures the boundary behavior of this solution, and in particular the exponential suppression between bulk and boundary amplitudes⁷.

We can compare this WKB approximation with the exact solution for $z = 2$ from section 3.2. Figure 4 shows a plot of the WKB solution for $z = 2$ Lifshitz, compared to the exact solution. As we can see, the WKB approximation accurately captures the exponential momentum-suppression at large α . (See also appendix A for further ‘benchmark tests’.) In the next section, we will use the WKB formalism to investigate for which spacetimes smearing functions exist.

4 Smearing Functions in Lifshitz spacetimes

In this section, we introduce smearing functions as a way to reconstruct bulk physics from boundary dynamics. Using the WKB formalism developed in appendix A, we will show that for Lifshitz spacetimes, and more generally for any flow involving Lifshitz, such reconstruction is not possible.

⁷Notice however that calculating the ratio B/A , which is needed to calculate the standard field theory Green’s function, would not be possible. This is due to the fact that for a general solution, the normalizable solution $\sim e^{-S}$ can ‘hide’ under the non-normalizable part $\sim e^S$, which grows much faster as $\rho \rightarrow 0$.

First, recall that the normalizable solutions of the Klein Gordon equation can be used to construct the Hilbert space of the bulk theory in the following way: We decompose the scalar as

$$\phi(t, \vec{x}, r) = \int dE d^d p \frac{1}{N_{E,p}} \left(\phi_{E,p}(t, \vec{x}, r) a_{E,p} + \phi_{E,p}^*(t, \vec{x}, r) a_{E,p}^\dagger \right), \quad (4.1)$$

where $a_{E,p}$ are operators, $N_{E,p} \equiv \langle \phi_{E,p}, \phi_{E,p} \rangle^{\frac{1}{2}}$ and $\langle \cdot, \cdot \rangle$ is the Klein-Gordon inner product, defined by

$$\langle f, g \rangle \equiv i \int_{\Sigma} d^d x dr \sqrt{-g} g^{00} (f^* \partial_t g - (\partial_t f^*) g). \quad (4.2)$$

Here, the integral is to be taken over a spacelike slice Σ .⁸

If we choose $\langle \phi_{E,p}, \phi_{E,p}^* \rangle = 0$, i.e. pick definite frequency solutions, the a and a^\dagger are the usual creation/annihilation operators for particles with wavefunction $\phi_{E,p}$. We can create all possible states in the Fock space by repeatedly acting with a^\dagger on the vacuum $|0\rangle_{\text{AdS}}$. In Lorentzian AdS/CFT, the bulk-boundary dictionary states that there exists a boundary operator defined by

$$O(t, \vec{x}) \equiv \lim_{r \rightarrow 0} r^{-\Delta_+} \phi(t, \vec{x}, r), \quad (4.3)$$

which is sourced by the classical, non-normalizable solution ϕ_{cl} behaving as r^{Δ_-} at the boundary. Taking the above limit in (4.1), we arrive at

$$O(t, \vec{x}) = \int dE d^d p \frac{1}{N_{E,p}} \left(\varphi_{E,p}(t, \vec{x}) a_{E,p} + \varphi_{E,p}^*(t, \vec{x}) a_{E,p}^\dagger \right). \quad (4.4)$$

Here $\varphi_{E,p} \equiv \lim_{r \rightarrow 0} r^{-\Delta_+} \phi_{E,p}$. The remarkable fact is that the boundary operator can be expanded in terms of *the same* a, a^\dagger as the bulk field. Thus, to create an arbitrary state in the bulk we can use either bulk operators or boundary operators that are ‘smeared’ over \vec{x} and t in an appropriate way. For example, for a single-particle state we have

$$a_{E,p} = \int dt' d^d x' N_{E,p} \varphi_{E,p}^*(t', \vec{x}') O(t', \vec{x}'), \quad (4.5)$$

so the state $|E, p\rangle_{\text{AdS}}$ can be built entirely out of boundary operators, and so on. Here we need to assume that the φ are normalized such that

$$\int dE d^d p \varphi_{E,p}^*(t, \vec{x}) \varphi_{E,p}(t', \vec{x}') = \delta(t - t') \delta(\vec{x} - \vec{x}'). \quad (4.6)$$

Notice that (4.6), and not (4.2), is the relevant inner product here. This is because the $\varphi_{E,p}$ are not solutions to any equation of motion at the boundary; rather, they are a set of complete functions⁹. The condition (4.6) is not in tension with the Klein-Gordon normalization condition in the bulk, since we have explicitly factored out $N_{E,p}$ in (4.1).

Equation (4.5) induces an isomorphism between the Fock-space representations of the bulk and boundary Hilbert spaces. The question we would like to answer is whether we can

⁸This norm accords with the norm preserved by the effective Schrödinger equation in (3.7).

⁹In other words: O is an off-shell operator.

express any operator in the bulk entirely in terms of boundary operators. In particular, we would like to reconstruct ϕ from its corresponding boundary operator O . We make the ansatz

$$\phi(t, \vec{x}, r) = \int dt' d^d x' K(t, \vec{x}, r | t', \vec{x}') O(t', \vec{x}'), \quad (4.7)$$

where K is called a smearing function. We can plug (4.5) back into (4.1) to obtain:

$$K(t, \vec{x}, r | t', \vec{x}') = \int dE d^d p \phi_{E,p}(t, \vec{x}, r) \varphi_{E,p}^*(t', \vec{x}'). \quad (4.8)$$

Note that this K differs from the usual bulk-to-boundary propagator in that it is a relationship among normalizable modes. Throughout this paper, we will assume that K has a well-defined Fourier transform, which allows us to interchange the order of integration above. We will comment on some mathematical details and the precise definition of K in section 6.

In Lifshitz spacetime, the normalizable solutions are given by

$$\phi_{E,p} = e^{-i(Et - \vec{p} \cdot \vec{x})} f_{E,p} = e^{-i(Et - \vec{p} \cdot \vec{x})} e^{-\frac{d}{2}B} \psi_{E,p}. \quad (4.9)$$

Near the boundary,

$$\psi \approx B_{E,p} \zeta^{\frac{1}{2} + \nu} \equiv \hat{B}_{E,p} r^{z(\frac{1}{2} + \nu)}, \quad (4.10)$$

so that

$$\varphi_{E,p} = \lim_{r \rightarrow 0} r^{-\Delta_+} \phi = e^{-i(Et - \vec{p} \cdot \vec{x})} \hat{B}_{E,p}. \quad (4.11)$$

The normalization condition (4.6) then requires $|\hat{B}_{E,p}| = (2\pi)^{-(d+1)/2}$. Let us now use the WKB approximation. For normalizable solutions, we have $C = 0$, or $a = -ib$, so the normalization of the wavefunction is fixed by

$$|b| = \nu^{\frac{1}{2}} z^{\frac{1}{2} + \nu} (2\pi)^{-\frac{d+1}{2}} \lim_{y \rightarrow 0} y^\nu e^{S(y)}. \quad (4.12)$$

The properly normalized WKB solution is then given by

$$\psi_{E,p}(\rho) = \begin{cases} (2\pi)^{-\frac{d+1}{2}} \nu^{\frac{1}{2}} z^{\frac{1}{2} + \nu} (U + \Delta U - E^2)^{-\frac{1}{4}} \lim_{y \rightarrow 0} y^\nu e^{S(y) - S(\rho)}, & \rho < \rho_0; \\ e^{i\frac{\pi}{4}} (2\pi)^{-\frac{d+1}{2}} \nu^{\frac{1}{2}} z^{\frac{1}{2} + \nu} (E^2 - U - \Delta U)^{-\frac{1}{4}} \lim_{y \rightarrow 0} y^\nu e^{S(y)} [e^{-i\Phi(\rho)} - ie^{i\Phi(\rho)}], & \rho > \rho_0, \end{cases} \quad (4.13)$$

where $S(\rho) = \int_\rho^{\rho_0} d\rho' \sqrt{U + \Delta U - E^2}$, $\Phi(\rho) = \int_{\rho_0}^\rho d\rho' \sqrt{E^2 - U - \Delta U}$ and $\Delta U \equiv 1/(2\rho')^2$ (see appendix A).

Using this result, we can write our candidate smearing function as

$$K = e^{-\frac{d}{2}B} \int \frac{dE}{(2\pi)^{\frac{1}{2}}} \frac{d^d p}{(2\pi)^{\frac{d}{2}}} e^{i(E(t' - t) - \vec{p} \cdot (\vec{x}' - \vec{x}))} \psi_{E,p}. \quad (4.14)$$

We recognize this integral as the inverse Fourier transform of $\psi_{E,p}$. We will now show that this object does not exist¹⁰ because ψ grows exponentially with momentum p .

¹⁰For a precise definition of what we mean by nonexistence, see section 6.

First, let E and ρ be fixed. We then choose p large enough so $\rho < \rho_0$, i.e. so the ρ we are considering is in the tunneling region. This choice is possible for any ρ . For concreteness, we can choose

$$p^2 > E^2 \rho^k. \quad (4.15)$$

Then

$$\left| \lim_{y \rightarrow 0} y^\nu e^{S(y)-S(\rho)} \right| = \lim_{y \rightarrow 0} y^\nu \exp \left(\int_y^\rho d\rho' \sqrt{\frac{\nu^2}{(\rho')^2} + \frac{p^2}{(\rho')^k} - E^2} \right), \quad (4.16)$$

and the integral is real-valued. Now let $0 < \lambda < 1$ such that $y < \lambda\rho < \rho$ and split the integral accordingly:

$$\int_y^\rho = \int_y^{\lambda\rho} + \int_{\lambda\rho}^\rho. \quad (4.17)$$

Roughly speaking, the first integral provides the boundary data with the correct asymptotic y -dependence, while the second integral is responsible for the exponential behavior in p . In the first integral, using (4.15), we find

$$\int_y^{\lambda\rho} d\rho' \sqrt{\frac{\nu^2}{(\rho')^2} + \frac{p^2}{(\rho')^k} - E^2} > \nu \log \left(\frac{\lambda\rho}{y} \right). \quad (4.18)$$

In the second integral, for p large enough¹¹ we can find a constant $0 < c < 1$ such that

$$\int_{\lambda\rho}^\rho d\rho' \sqrt{\frac{\nu^2}{(\rho')^2} + \frac{p^2}{(\rho')^k} - E^2} > \int_{\lambda\rho}^\rho d\rho' \frac{cp}{(\rho')^{\frac{k}{2}}} = cz\rho^{\frac{1}{z}} \left(1 - \lambda^{\frac{1}{z}} \right) p. \quad (4.19)$$

Putting everything together, we conclude that for E and ρ fixed, there exist $c, \lambda \in (0, 1)$ and p_0 such that

$$\left| \lim_{y \rightarrow 0} y^\nu e^{S(y)-S(\rho)} \right| > (\lambda\rho)^\nu \exp \left[cz\rho^{\frac{1}{z}} (1 - \lambda^{\frac{1}{z}}) p \right], \quad (4.20)$$

for all $p > p_0$. Hence the function $\psi_{E,p}$ grows exponentially with p and the smearing function defined in (4.8) does not exist¹².

The inability to construct a smearing function is due to the existence of trapped modes, which have to tunnel through V_p to reach the boundary. The boundary imprint of these modes is suppressed by a factor of e^{-cp} , where c is some positive constant depending on the geometry. However, the normalization condition (4.6) turns this suppression into an exponential amplification: For any given mode the smearing function takes the corresponding boundary data and amplifies it by an appropriate factor to reconstruct bulk information. Consequently, trapped modes receive a contribution e^{+cp} in the smearing function integral. As $p \rightarrow \infty$, the boundary imprint of trapped modes becomes arbitrarily small, and as a result the smearing function integral diverges.

¹¹For concreteness, choose e.g. $p^2 > E^2 \rho^k / (1 - c^2)$.

¹²This exponential behavior in p is distinct from the behavior of $|B|/|b|$ in α (see e.g. (3.31)), since here we are interested in the amplitude of the wavefunction at a fixed radial location ρ , and not its overall normalization.

The splitting of the domain of integration into a near-boundary region $[0, \lambda\rho]$ and a bulk region $[\lambda\rho, \rho]$ is crucial for our proof: In the near-boundary region, we use the fact that no matter how large p is, we can make ρ' small enough such that the cosmological- and mass-terms in the potential dominate over V_p and we can approximate $U \approx \nu^2/(\rho')^2$. Modes that tunnel through this part do not contribute an exponential factor $\sim e^p$, but rather produce the correct boundary scaling $y^{-\nu}$. This scaling is consequently stripped off by the y^ν factor in (4.16). In the bulk region near ρ , however, there is a minimum value that ρ' can take, so as we drive p to infinity, eventually $U \approx p^2/(\rho')^k$ becomes a very good approximation. This is what produces the exponential factor in (4.20).

We see that there are two qualitatively different limits of the potential: $\rho \rightarrow 0$ and $p \rightarrow \infty$. Both of them are important for understanding the behavior of (4.16), which is why we need to pick $0 < \lambda < 1$ to get a lower bound that reflects this behavior. Simply setting $\lambda = 0$ corresponds to approximating $U \approx p^2/(\rho')^k$ everywhere. However, in doing so we would be neglecting the boundary scaling $y^{-\nu}$, and consequently the lower bound (4.20) would be zero. Similarly, $\lambda = 1$ corresponds to approximating $U \approx \nu^2/(\rho')^2$ everywhere. While this is certainly true for small ρ' , we would be missing the fact that the momentum part V_p of the potential can still dominate in any interval away from the boundary (i.e. close to ρ) and lead to exponential growth. The bound (4.20) would just be a constant independent of p and we would not be able to make the same conclusion about the smearing function.

4.1 Momentum-space analysis

It is instructive to analyze the behavior of the integral (4.14) at large momenta in the $(E, |p|)$ -plane. We already saw that for fixed energy E , the smearing function diverges exponentially with $|p|$, as the tunneling barrier becomes arbitrarily large at high momenta. However, this is not necessarily the only direction along which the integral diverges. Let us introduce polar coordinates

$$\begin{aligned} |p| &= q \cos \theta \\ E &= q \sin \theta. \end{aligned} \tag{4.21}$$

Figure 5 shows a sketch of the spectrum in the $(E, |p|)$ -plane: The solid line divides trapped modes, which have to tunnel through V_p from ‘free’ modes, which only tunnel through $U \sim 1/\rho^2$. If we imagine cutting off Lifshitz at some small value $\lambda\rho$ with $\lambda < 1$, all modes with $E < (\lambda\rho)^{-\frac{1}{2}} |p|$ (yellow region) are trapped modes¹³. Let us study the integral which defines the smearing direction. If we perform this integral along any direction θ over these modes (i.e. $\tan \theta < (\lambda\rho)^{-\frac{1}{2}}$), the exponential term in the integrand behaves as

$$\text{Re}(S(y) - S(\rho)) = \int_y^\rho d\rho' \sqrt{\frac{\nu_z^2}{(\rho')^2} + \left(\frac{1}{(\rho')^k} - \tan^2 \theta\right) q^2 \cos^2 \theta}. \tag{4.22}$$

¹³Notice that the choice of λ is arbitrary. In particular, along any line $E = \tan \theta |p|$, there is a choice of λ such that all modes are below the momentum-barrier for large enough $|p|$. Nevertheless, because of the subtleties discussed at the end of the previous section, we should not simply take $\lambda \rightarrow 0$ but instead work with a small but finite value.

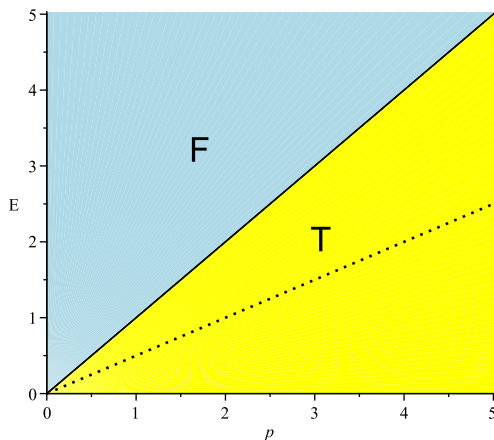


Figure 5. Sketch of free (F) and trapped (T) modes for general case. Deforming the geometry in the IR may introduce a cutoff (dotted line), but this line will always remain below the solid line, and some trapped modes survive.

For q large enough, this term grows linearly and the smearing function is exponentially divergent. We see that the variable that controls the suppression (or amplification) due to tunneling is in fact $q = \sqrt{E^2 + p^2}$, as opposed to just $|p|$.

4.2 No smearing function \Leftrightarrow singularities?

The divergence of the smearing function is due to trapped modes, which correspond to classical geodesics that cannot reach the boundary. However, those are precisely the trajectories that start and end at the tidal singularity at $\rho \rightarrow \infty$, so their fate is not well-understood even on the classical level. Therefore, one might wonder if the inability to construct smearing functions is simply due to the presence of singularities. This question has been raised before in the case of black hole solutions in AdS¹⁴ [38, 39]. Fortunately, in our case there are known ways to resolve the singularity, so we can directly test the conjecture that non-existence of smearing functions is related to singularities.

In the context of Einstein-Maxwell-dilaton systems [24], the Lifshitz singularity can be resolved by including corrections to the dilaton effective potential. For magnetically charged branes, the dilaton runs towards strong coupling in the IR. Using a toy-model of the quantum corrected action, the authors of [21] showed that the Lifshitz geometry can be resolved into an $\text{AdS}_2 \times \mathbb{R}^2$ region in the deep IR. For electrically charged solutions, the dilaton runs towards weak coupling near the horizon, and higher derivative corrections become important. In [23], two of the current authors showed that by coupling the dilaton to higher curvature terms in an appropriate way, the singularity can be resolved in a similar fashion. In particular,

¹⁴However, we should point out that the two types of singularities encountered here are qualitatively different. In the Lifshitz case, the singularity is ‘mild’, in the sense that all curvature invariants remain finite. It is, however, felt by strings that fall towards the horizon [41].

numerical solutions were constructed that interpolate between AdS_4 in the UV to Lifshitz in some intermediate regime, and finally to $\text{AdS}_2 \times \mathbb{R}^2$ in the deep IR. We would like to use these numerical flows to test whether resolving the singularity can make the smearing function well-defined.

As a warm-up, consider the following analytical toy-model describing such a flow:

$$\begin{aligned} e^{2A} &= \frac{1}{\rho^2}, \\ e^{2B} &= \begin{cases} \frac{1}{\rho^2}, & 0 < \rho < R_1; \\ \frac{1}{R_1^k \rho^{2-k}}, & R_1 < \rho < R_2; \\ \frac{1}{R_1^k R_2^{2-k}}, & R_2 < \rho, \end{cases} \\ C &= A. \end{aligned} \tag{4.23}$$

The last condition is a gauge choice, which fixes our radial coordinate to be ρ , as defined in (3.4). The potential is given by

$$U(\rho) = \begin{cases} \frac{\nu_1^2 - \frac{1}{4}}{\rho^2} + p^2, & 0 < \rho < R_1; \\ \frac{\nu_z^2 - \frac{1}{4}}{\rho^2} + p^2 \left(\frac{R_1}{\rho} \right)^k, & R_1 < \rho < R_2; \\ \frac{\nu_\infty^2 - \frac{1}{4}}{\rho^2} + p^2 \left(\frac{R_1}{R_2} \right)^k \left(\frac{R_2}{\rho} \right)^2, & R_2 < \rho, \end{cases} \tag{4.24}$$

where ν_z was defined in (3.15), and $0 < k < 2$. All modes with $p > E$, or equivalently $\tan \theta < 1$ are trapped. It is interesting to note that since the potential goes to zero as $\rho \rightarrow \infty$, there are now modes that are below the barrier in the AdS_{d+2} region. For pure AdS, this is not possible, as the wavefunction cannot be below the barrier everywhere.

Let us see if a smearing function exists for any point ρ in the bulk. For $0 < \rho < R_1$, we need to compute

$$\left| \lim_{y \rightarrow 0} y^\nu e^{S(y) - S(\rho)} \right| = \lim_{y \rightarrow 0} y^\nu \exp \left(\text{Re} \int_y^\rho d\rho' \sqrt{\frac{\nu_1^2}{\rho'^2} + (1 - \tan^2 \theta) q^2 \cos^2 \theta} \right). \tag{4.25}$$

Naively, one might expect that since we are integrating all the way up to the boundary at $\rho = 0$, the $1/\rho^2$ -term will eventually dominate and there is no q -divergence. However, we have seen before that it is necessary to split the integral into a near-boundary region and a bulk region, according to (4.17). The near boundary integral will then produce the typical boundary scaling $y^{-\nu}$, while the bulk integral will grow linearly for trapped modes. In complete analogy with (4.20) we find that there exist constants $q_0, c > 0$ and $\lambda \in (0, 1)$ such that

$$\left| \lim_{y \rightarrow 0} y^{\nu_1} e^{S(y) - S(\rho)} \right| > (\lambda r)^{\nu_1} e^{cq},$$

for all $q > q_0$. Again, even though the $1/\rho^2$ part of the potential dominates near the boundary, there is still an exponential divergence due to trapped modes, and the smearing function does not exist in the AdS region.

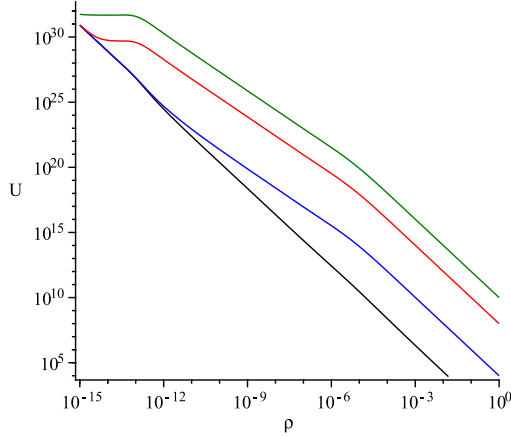


Figure 6. Effective potential U for the numerical flow found in [23], for $m = 1$. The momentum increases from bottom to top, with $p = 0$ (black), 10^2 (blue), 10^4 (red), 10^5 (green). At large momenta, the potential is well approximated by $V_p = e^{2W} p^2$.

For points within the Lifshitz region ($R_1 < \rho < R_2$), the relevant integral contains an integral over the AdS_{d+2} region, which is divergent by itself, plus an additional term

$$\int_{R_1}^{\rho} d\rho' \sqrt{\frac{\nu_z^2}{\rho'^2} + \left(\left(\frac{R_1}{\rho'} \right)^k - \tan^2 \theta \right) q^2 \cos^2 \theta}. \quad (4.26)$$

This integral gives a real contribution for $\tan \theta < (R_1/\rho)^{k/2}$, which grows linearly with large q . Hence the smearing function still grows like $e^{c'q}$, but now $c' > c$ and it diverges even faster than in the AdS_{d+2} part.

The same logic can be applied to a point within the $\text{AdS}_2 \times \mathbb{R}^d$ region in the IR ($\rho > R_2$). In this case there is a contribution from both AdS_{d+2} and Lifshitz, plus a contribution

$$\int_{R_2}^{\rho} d\rho' \sqrt{\frac{\nu_{\infty}^2}{\rho'^2} + \left(\left(\frac{R_1}{R_2} \right)^k \left(\frac{R_2}{\rho'} \right)^2 - \tan^2 \theta \right) q^2 \cos^2 \theta}. \quad (4.27)$$

Modes with $\tan \theta < (R_1/R_2)^{k/2} R_2/\rho$ begin to tunnel already in the $\text{AdS}_2 \times \mathbb{R}^d$ part of the potential, and so the smearing function will diverge even faster at large q . The final result is that there is no smearing function for any point ρ in the bulk. The trapped modes lead to an exponential divergence which becomes worse the deeper we try to reach into the bulk.

Let us now check that the result obtained for the toy-model (4.23) is indeed correct also for the exact numerical solution found in [23] (here $d = 2$). The effective potential is plotted in Figure 6. As p increases, the potential becomes better and better approximated by V_p (shown in Figure 7). The metric coefficients and potential are of the form given in (4.23) and (4.24), except that now there is a smooth transition between the three regions.

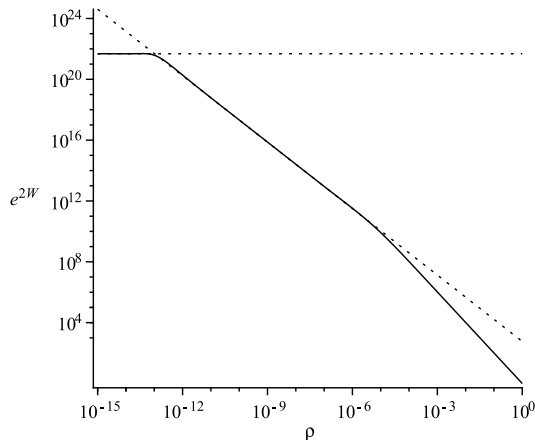


Figure 7. The factor e^{2W} for the same numerical solution. The solution flows from AdS_4 ($e^{2W} \approx \text{const.}$), to Lifshitz ($e^{2W} \sim \rho^{1.45}$, corresponding to $z \approx 3.68$) to $\text{AdS}_2 \times \mathbb{R}^2$ ($e^{2W} \sim \rho^{-2}$).

Figures 8-10 show the real part of $S(y) - S(\rho)$ in the $(E, |p|)$ -plane. Instead of taking y to zero we choose $y \approx 10^{-15}$, which we may think of as disregarding the near-boundary region of the ρ' -integral and starting at $y = \lambda\rho$. The thick line divides free (blue) modes from trapped (yellow) modes. The contours represent lines along which $\text{Re}(S(y) - S(\rho))$ is constant. If we keep E fixed and increase p , we cross the contours at approximately equal distances, so the integral grows linearly in p . This is not only true for lines of constant E , but for any line within the trapped region (i.e. any line that stays below the black solid line). Hence the integral indeed diverges linearly with $q = \sqrt{E^2 + p^2}$, as was anticipated in section 4.1.

Figure 11 shows $\text{Re}(S(y) - S(\rho))$ for three points representing AdS_4 , Lifshitz and $\text{AdS}_2 \times \mathbb{R}^2$. The energy is held fixed at $E = 10^{16}$, such that at small p , the wavefunction is oscillating everywhere. As we increase p , the mode eventually becomes trapped and the real part of the integral grows linearly. Note that in the log-log plot used here, the three curves lie nicely on top of each other. This fact confirms our prediction that the smearing function diverges faster the deeper we try to reach into the bulk.

We conclude that resolving the tidal singularity is not enough to make the smearing function well defined. The $\text{AdS}_2 \times \mathbb{R}^2$ region in the IR can be thought of as the $z \rightarrow \infty$ limit of Lifshitz spacetime. As a consequence, $V_p \sim \rho^{-2}$, and there are still trapped modes with arbitrarily small boundary imprint.

It is also worth commenting on the addition of an AdS region in the UV, as in (4.23), which may seem desirable to make the holographic renormalization procedure better-defined. We have seen explicitly that the integral over (4.25) is still divergent at large momenta and a smearing function does not exist, even for points close to the boundary. This is the quantum equivalent of the observation made at the end of section 2.1, that null geodesics with large enough p still see a ‘Lifshitz barrier’ and remain trapped inside the bulk, regardless of the near-boundary geometry.

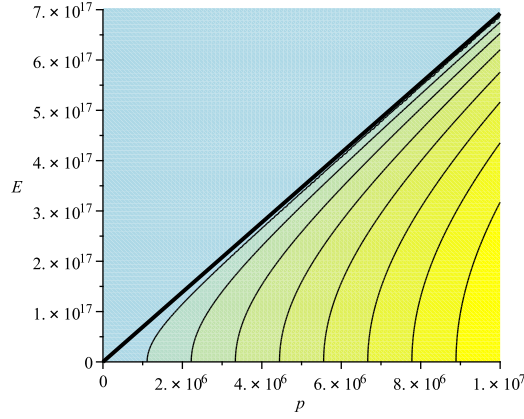


Figure 8. Plot of $\text{Re}(S(y) - S(\rho))$ for a point within the AdS_4 region ($\rho \approx 1.3 \cdot 10^{-15}$). The black solid line represents $V_p = E^2$ and divides free (blue) from trapped modes (yellow). Contours indicate lines of constant $\text{Re}(S(y) - S(\rho))$, with a linear increase between different contours.

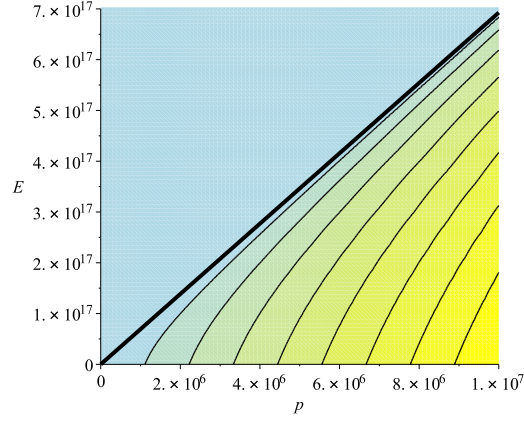


Figure 9. Plot of $\text{Re}(S(y) - S(\rho))$ for a point within the Lifshitz region ($\rho \approx 9 \cdot 10^{-8}$).

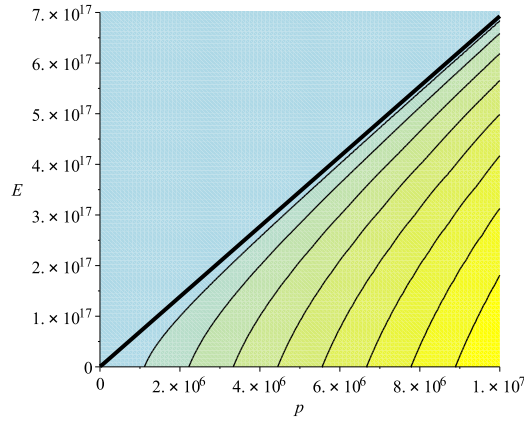


Figure 10. Plot of $\text{Re}(S(y) - S(\rho))$ for a point within the $\text{AdS}_2 \times \mathbb{R}^2$ region ($\rho \approx 1$).

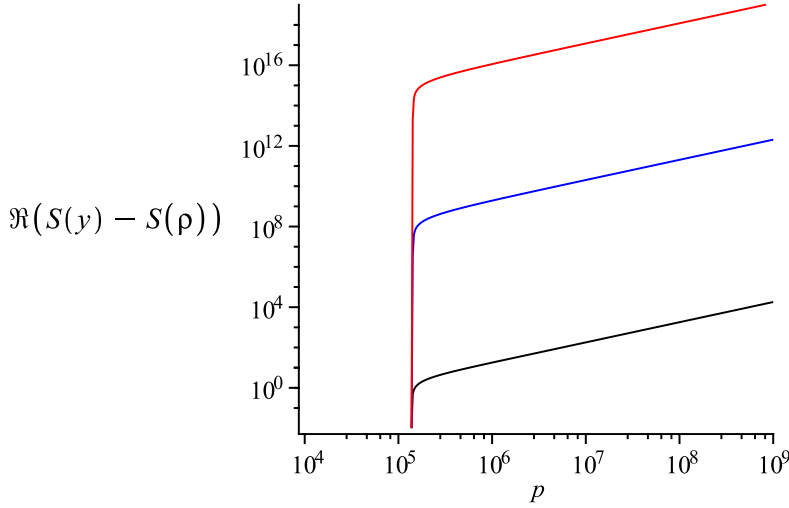


Figure 11. Plot of the real part of $S(y) - S(\rho)$ vs. p at three different positions within the AdS_4 ($\rho \approx 1.3 \cdot 10^{-15}$), Lifshitz ($\rho \approx 9 \cdot 10^{-8}$) and $\text{AdS}_2 \times \mathbb{R}^2$ ($\rho \approx 1$) regions (from bottom to top). The energy is fixed at $E = 10^{16}$ and we chose $m = 1$. For large momenta, the solution begins to tunnel and contributes an exponential factor in K .

4.3 Other flows involving Lifshitz

The $\text{AdS}_2 \times \mathbb{R}^d$ geometry considered in the previous section is not the only possible IR endpoint of the RG-flow for Lifshitz solutions. Ref. [18–20] have considered flows from Lifshitz in the IR to an AdS_{d+2} fixed point in the UV. These flows are of particular interest to us, since V_p does not go to zero as $\rho \rightarrow \infty$, but reaches a constant value corresponding to the AdS geometry at the horizon. Consequently, some of the problematic trapped modes never oscillate, and are thus removed from the spectrum. To see how this works, consider the following toy-model of such a Lifshitz to AdS_{d+2} flow:

$$\begin{aligned}
 e^{2A} &= \frac{1}{\rho^2}, \\
 e^{2B} &= \begin{cases} \frac{1}{\rho^{2-k}}, & 0 < \rho \leq R_1; \\ \frac{R_1^k}{\rho^2}, & \rho > R_1, \end{cases} \\
 C &\equiv A.
 \end{aligned} \tag{4.28}$$

The potential is given by

$$U(\rho) = \begin{cases} \frac{\nu_z^2 - \frac{1}{4}}{\rho^2} + \frac{p^2}{\rho^k}, & 0 < \rho \leq R_1; \\ \frac{\nu_1^2 - \frac{1}{4}}{\rho^2} + \frac{p^2}{R_1^k}, & \rho > R_1. \end{cases} \tag{4.29}$$

To compute the smearing function at some fixed $\rho \leq R_1$ we again split the interval $[0, \rho]$ into a near-boundary region $[0, \lambda\rho]$ and a bulk region $[\lambda\rho, \rho]$, where $\lambda < 1$. In the bulk region,

the potential can be approximated by $V_p = p^2/\rho^k$ for p large enough. Then, modes with $p > (\lambda\rho)^{k/2}E$ are trapped by V_p . For $\rho > R_1$, the potential takes a constant value. In pure Lifshitz, modes with $p < R_1^{k/2}E$ would have been oscillating in this region. However, these modes are now completely under the barrier and therefore have to be excluded from the spectrum. The AdS_{d+2} region in the IR thus introduces a natural (energy-dependent) momentum cutoff.

Nevertheless, there is still a finite wedge of trapped modes with $R_1^{-k/2} < \tan\theta < (\lambda\rho)^{-k/2}$ (cf. Figure 5) and integrating up to $q = \infty$ will produce the same divergent behavior as before. In section 5.1, we will give a general argument as to why this has to be the case, and show that no smooth IR-deformation can remove all trapped modes from the spectrum.

5 Generalization

We have seen that the construction of smearing functions can fail if there are modes that have to tunnel through a momentum barrier in the potential. The integral (4.8) diverges if such modes exist at arbitrarily large $q = \sqrt{E^2 + p^2}$. In this section, we will generalize our previous findings to prove that smearing functions do not exist for any geometries that allow trapped modes.

Consider a background that satisfies

$$\partial_\rho e^W < 0 \text{ for } \rho \in [\rho_1, \rho_2]. \quad (5.1)$$

We would like to compute the smearing function at a bulk point $\rho > \rho_1$. All modes with $V_p(\rho_1) > E^2$ have to tunnel through some part of V_p and are therefore trapped modes. Let us write the integral defining the smearing function in (4.8) as $\int dE d|p| \int d\Omega_{d-1}$ and focus on the integral in the $(E, |p|)$ -plane. The domain of integration is shown in Figure 5, where free and trapped modes are separated by the solid line $E^2 = V_p(\rho_1)$. Choosing polar coordinates (4.21), we find that the exponential part of the integrand satisfies

$$\text{Re}(S(y) - S(\rho)) > \text{Re} \int_{\rho_1}^{\rho_2} d\rho' \sqrt{V_m(\rho') + V_{\cos}(\rho') + (e^{2W(\rho')} - \tan^2\theta) \cos^2\theta q^2}$$

Since the integration domain does not include the boundary, the first two terms under the square root are bounded. Thus, for $\tan\theta < e^{W(\rho_1)}$, the integral grows linearly with large q and the smearing function diverges exponentially. The divergence appears not only at fixed E , but under any angle in the yellow region of Figure 5.

Consequently, if a geometry has trapped modes that are below the barrier at some ρ_1 , a smearing function does not exist for any $\rho > \rho_1$. From the null energy condition (2.6) and the discussion thereafter, we know that once $\partial_\rho e^W$ is negative for some ρ_1 , it cannot be positive for any $\rho < \rho_1$. Thus, once the wavefunction is below the V_p barrier, it will stay below it as we go towards the boundary. Using the terminology introduced in section 2, trapped modes cannot become free near the boundary. Therefore, when computing the smearing function

$K(t, x, \rho|t', x')$, there is an exponential contribution from trapped modes regardless of which bulk point ρ we consider.

The condition (5.1) makes it is easy to identify geometries without smearing functions. Clearly, Lifshitz has $\partial_\rho e^W < 0$ everywhere, and as we saw earlier, K does not exist. If we instead consider flows that involve only a finite region with broken Lorentz invariance, such that (5.1) is satisfied in some region, we still have trapped modes, and the smearing function will not exist. This analysis includes flows involving a Lifshitz region, as well as hyperscaling geometries with Lifshitz scaling. Our analysis above shows that none of these geometries admit smearing functions, provided the spacetime satisfies the NEC.

5.1 Removing trapped modes via deformations

In our discussion above, we always assumed that the momentum-space integral (4.8) does in fact include trapped modes with arbitrarily large q on some set of nonzero measure. This is clearly the case in the examples mentioned above. On the other hand, the smearing function for AdS converges because modes with $p^2 > E^2$ are simply not part of the spectrum, as the corresponding wavefunction would have to be below the potential globally.

One might wonder if it is possible to ‘fix’ a geometry which a priori does not admit a smearing function, by removing all trapped modes from the spectrum in a physical way. The AdS example gives us a hint on how one might accomplish this task: If the geometry is deformed in the deep IR such that would-be trapped modes never actually oscillate, they would simply not be allowed.

Following our discussion of the null energy condition in section 2, it follows that there are only three relevant IR asymptotics that we need to consider:

1. e^W decreases monotonically to a constant value $\mu > 0$.
2. e^W attains a minimum value $\mu > 0$, but then goes to constant $M > \mu$.
3. e^W attains a minimum value $\mu > 0$, but then goes to infinity.

Trapped states are equivalent to tunneling states in the potential $V_p = p^2 e^{2W}$. For p large enough, these states always exist [51]. This can be seen heuristically by bounding the potential from above with an appropriate square-well potential $\tilde{U}(\rho)$ (see Figure 12). Therefore, no smooth deformation can ever remove all trapped modes from the spectrum.

As an example, consider case 1, which captures the case of the Lifshitz to AdS_{d+2} flow discussed in section 4.3. The AdS region introduces an energy-dependent momentum cutoff $p < E/\mu$. However, since μ is by definition a global minimum and (5.1) holds, we clearly have $\mu < e^{W(\rho_1)}$. Although the cutoff may remove some trapped modes from the spectrum, there will always remain a wedge of trapped modes that gives a divergent contribution when integrated over (see Figure 5). We conclude that spaces without a smearing function cannot be deformed smoothly to make the smearing function well-defined.

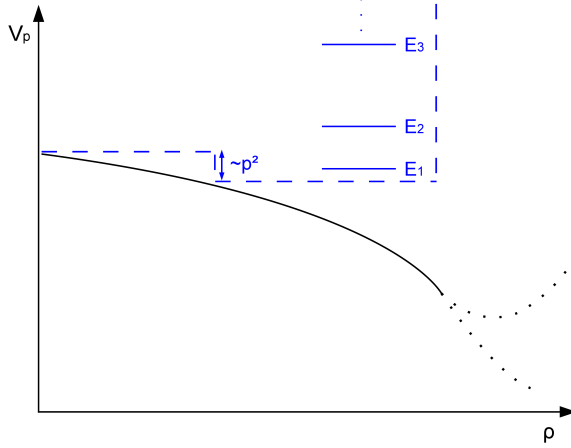


Figure 12. Sketch of V_p for a potential satisfying (5.1). This includes deformations of AdS and flows involving Lifshitz. Using the min-max principle, the energy levels are bounded from above by those of a square-well potential. In the large p limit, there are always trapped modes. The near-horizon behavior of the potential is irrelevant for our discussion.

5.2 Adding trapped modes via deformations

Another interesting question is what happens if we take a geometry with a smearing function, such as AdS [32–34], and add a small (planar) perturbation in the IR. It can be seen from (2.6) that e^W must start with non-positive slope at the boundary for any background that is asymptotically AdS¹⁵. Since the potential scales with p , such a perturbation will always introduce new trapped modes. In particular, the momentum-potential $V_p = p^2 e^{2W}$ can always be bounded from above by a semi-infinite square-well potential of width l and height $h = p^2 h_0$, where h_0 is some constant (see Figure 12). For large enough p , the square-well always admits bound states with $p^2(1 - h_0) < E^2 < p^2$ and, via the min-max principle, so will V_p . As a result, the smearing function would be destroyed anytime the metric is deformed by such a perturbation.

This result is interesting, as it opens up the possibility that ‘small’ perturbations of AdS can make the smearing function ill-defined by introducing new trapped states. However, we should keep in mind that our ansatz only allows for planar perturbations; we cannot consider localized disturbances. It would be interesting to study the effect of such perturbations in a more general setup. Again, notice that the ultimate IR fate of the geometry with AdS behavior in the UV is not important for this discussion. In particular, whether or not there is a singularity at $r \rightarrow \infty$ does not change the qualitative result.

¹⁵ If we do not insist on AdS asymptotics, then we could choose e^W to immediately have a positive slope. If e^W has positive slope at some ρ_+ , the NEC dictates that e^W cannot begin to decrease at some larger ρ . Thus, in this scenario no trapped modes are introduced, and the smearing function will continue to exist everywhere. In particular, we cannot have a situation akin to Figure 5 in [39], where the potential has a dip allowing trapped modes to become oscillating again close to the boundary.

5.3 Relativistic domain wall flows

Given the above considerations, one may get the impression that the smearing function no longer exists for any geometry other than pure AdS. However, it is important to realize that such a conclusion is in fact unwarranted. What we have seen is that the non-existence of the smearing function is intimately tied to the presence of trapped modes with exponentially small imprint on the boundary. Since such modes arise from the large p limit of $V_p = e^{2W} \vec{p}^2$, they are naturally absent when $W = 0$, corresponding to flows preserving $(d+1)$ -dimensional Lorentz symmetry

$$ds_{d+2}^2 = e^{2B(r)}[-dt^2 + d\vec{x}_d^2] + e^{2C(r)}dr^2. \quad (5.2)$$

In this case, the Schrödinger equation (3.7) is more naturally written as

$$-\psi'' + (V_m + V_{\cos})\psi = (E^2 - \vec{p}^2)\psi. \quad (5.3)$$

In particular, the effective potential $\hat{U} = V_m + V_{\cos}$ no longer scales with p .

In general, \hat{U} may admit bound states and/or modes trapped at the horizon. Although bound states fall off exponentially outside the classically allowed region, since such states occur only at fixed values of $Q^2 \equiv E^2 - \vec{p}^2$, they will always have a non-vanishing (although small) amplitude at the boundary. Hence the presence of such states do not present an obstruction to the existence of a smearing function. Trapped modes at the horizon, on the other hand, are potentially more troubling, as they may form a continuum spectrum with a limit of vanishing amplitude on the boundary. However, it turns out that this possibility does not prevent the construction of a well-defined smearing function $K(t, x, r|t', x)$ for any fixed value of r . The point here is that since \hat{U} is independent of Q , the maximum suppression factor to tunnel from the boundary to r is bounded by setting $Q = 0$ in (5.3). As a result, it is impossible to make the suppression arbitrarily small. Hence we conclude that the smearing function exists for finite r in the case of relativistic domain wall flows, although the $r \rightarrow \infty$ limit of K may not exist if there are trapped modes that live arbitrarily far from the boundary.

We see that it is generally possible to define a smearing function only for relativistic flows, where $W = 0$ along the entire flow. Furthermore, for the case of $\text{AdS}_{d+2} \rightarrow \text{AdS}_{d+2}$ flows, the effective potential \hat{U} falls off as $1/\rho^2$ both in the UV and the IR. Since this potential is too steep to admit trapped modes in the deep IR, there are no modes completely removed from the boundary, and hence the $r \rightarrow \infty$ limit of the smearing function is well-defined. Thus in this case the entire bulk may be reconstructed.

6 Modifying the bulk-boundary dictionary

We have seen that for transverse Lorentz-breaking spacetimes with locally decreasing transverse speed of light, the smearing function is not well defined, even after resolving potential singularities. Thus, we are left with the option of loosening some of our initial assumptions about this function and its corresponding entry in the bulk-boundary dictionary. In particular, we need to reexamine our implicit assumption that K can reconstruct the bulk up to arbitrarily small transverse length scales.

Let us be a bit more precise about what kind of mathematical object the smearing function really is, and what we mean by saying that K does or does not exist. The most general possible definition is to let the smearing function be any map from boundary operators to bulk fields. However, a reasonable condition is that K defines a continuous, linear functional on the space of boundary operators. Continuity means that for any convergent sequence of boundary operators O_n we have

$$\lim_{n \rightarrow \infty} K [O_n] = K \left[\lim_{n \rightarrow \infty} O_n \right]. \quad (6.1)$$

The difficulty in constructing such a K is due to the fact that the two limits are defined with respect to very different norms. The bulk norm relevant for the left hand side is the Klein-Gordon norm (4.2), while the boundary norm for O is given by (4.6). We have seen that in spacetimes with $\partial_\rho e^W < 0$ locally, there exist nonzero bulk solutions that have exponentially small boundary imprint, which provide an obstruction for constructing continuous smearing functions.

Our strategy in this paper was to calculate a candidate smearing function \hat{K} in momentum space, and ask whether it defines a well-behaved object in position space. The problematic case is when the function defined in this way grows exponentially, i.e. $\hat{K} \approx e^{cp}$. Its action on a boundary field can be written in momentum space as

$$K [O] \sim \int dp \hat{K} (p) \hat{O} (p). \quad (6.2)$$

Whether or not this integral is well-defined clearly depends on what we allow \hat{O} to be: If \hat{O} is a square-integrable function, the smearing function has to be square-integrable as well, which is clearly not the case here.

What if we impose a stricter fall-off condition at $p \rightarrow \infty$? One rather strict condition would be that \hat{O} falls off faster than any inverse power of p at infinity¹⁶. A classic example of such a function is a Gaussian $\sim e^{-p^2}$. However, e^{cp} is not a well-defined functional on this space either. This can be seen by explicitly constructing a sequence of functions with ‘arbitrarily small’ boundary imprint, i.e. a sequence that goes to zero in the boundary norm. For example, consider

$$\hat{O}_n (p) \equiv e^{-cn} \Psi (p - n), \quad (6.3)$$

where Ψ is some bump-function. Attempting to reconstruct the corresponding bulk solution yields $K[O_n] \sim \int dp \Psi (p)$, which is independent of n , and in particular never equal to zero. Using (6.1), this means that the smearing function is not continuous.

The only way to make sense of the smearing function is to completely avoid configurations with arbitrarily small boundary imprint. This can only be achieved by introducing a hard momentum cutoff Λ . In other words, we attempt to invert the bulk-boundary map $\phi \mapsto O$ only for configurations with $\hat{O}(p > \Lambda) = 0$. Acting on these functions, the exponential e^{cp} is indeed a well-defined continuous functional, and the integral (6.2) converges. There is,

¹⁶In other words: O is a Schwartz-function and K is a tempered distribution.

however, a price to pay: as is well-known, the Fourier transform of such compactly supported functions does not have compact support. The position space wavefunction necessarily has to ‘leak out’ to infinity, and thus full localization in the transverse direction can never be achieved¹⁷.

7 Conclusion

Motivated by some of the difficulties that have been observed in trying to understand the global structure of Lifshitz spacetimes, we have studied the possibility of bulk reconstruction from the boundary information. At the classical level, the presence of non-radial null geodesics that do not reach the Lifshitz boundary suggests that much of the bulk data is inaccessible from the boundary. We have confirmed this heuristic picture by studying smearing functions for a bulk scalar field and demonstrating that they do not exist for Lifshitz spacetimes with $z > 1$. The reason for this is that there will always be trapped modes in the bulk that have exponentially vanishing imprint on the boundary. It is these modes and the information that they contain that cannot be reconstructed from any local boundary data.

Of course, it is well known that a pure Lifshitz background has a tidal singularity at the horizon. Since the trapped modes begin and end in the tidal singularity, we had initially conjectured that resolving the Lifshitz singularity would remove such modes and lead to a well defined smearing function. However, this is not the case, as we have seen; even with a regular horizon such as $\text{AdS}_2 \times \mathbb{R}^d$ or AdS_{d+2} , there will be trapped modes with vanishing imprint on the boundary as the transverse momentum is taken to infinity. Thus the existence or non-existence of a smearing function is independent of the nature of the horizon, and in particular whether it is singular or not.

More generally, we have seen that the constructibility of the smearing function depends crucially on whether there exists a family of trapped modes with arbitrarily small suppression on the boundary. The only way this can arise is if the momentum dependent part of the effective Schrödinger potential $V_p = e^{2W} \vec{p}^2$ has a local minimum or a barrier that grows as $p \rightarrow \infty$. Thus the question of whether the smearing function exists is closely related to the behavior of the gravitational redshift factor e^{-W} . In general, all non-relativistic backgrounds such as Lifshitz and ones with hyperscaling violation (including flows with such regions) do not admit smearing functions. The same is true for geometries such as Schwarzschild-AdS, where e^{2W} starts out as unity on the boundary, but vanishes at the horizon [39]. On the other hand, smearing functions are expected to exist for backgrounds with $W = 0$, i.e. ones preserving $(d + 1)$ -dimensional Lorentz invariance along the entire flow.

The scaling of V_p with \vec{p}^2 has the important consequence that any trapped mode will always be completely suppressed on the boundary with a factor $\sim e^{-cq}$ as $q \rightarrow \infty$, where $q^2 = E^2 + \vec{p}^2$ and c is a geometry and radial location dependent positive constant. This gives

¹⁷Here we have taken the necessity of smearing ϕ in position space as an indication of nonlocality. However, from a quantum point of view, a more proper indication of nonlocality would be the nonvanishing of the commutator outside of the lightcone.

rise to the perhaps somewhat unexpected feature that, with the existence of trapped modes, the smearing function $K(t, x, r|t', x)$ cannot exist even in an asymptotic AdS_{d+2} region near the boundary, so long as r is at a fixed location. One may wonder why the presence of trapped modes living in the IR would destroy the possibility of reconstruction of the UV region near the boundary. The reason for this is that, while a trapped mode in the IR indeed has to tunnel to reach the boundary, its amplitude does not immediately vanish in the interior of the bulk geometry. Moreover, these modes can live at a finite distance from the boundary. Hence they can have an imprint at any fixed r in the bulk, and yet vanish on the boundary. It thus follows that the bulk information corresponding to such modes cannot be obtained from the boundary, and thus the smearing function would not exist for any fixed value of r .

Since the existence of trapped modes with arbitrarily large values of q provides an obstruction to the construction of a smearing function, one way around this difficulty is to remove such modes by considering a hard momentum cutoff Λ . Another way to think about this is that it may indeed be possible to reconstruct the bulk data from the boundary information, but only up to a fixed momentum Λ . As Λ is taken larger, the reconstruction becomes more difficult, as there would be larger amplification in going from the boundary to the bulk due to the presence of trapped modes with larger values of q . With such a cutoff, one would have good control of the near boundary region in the bulk. However, one would lose complete localization in the transverse directions.

Finally, let us try to give at least a partial answer to the question raised in the title of this paper. If we limit ourselves to a minimum spatial resolution, local operators in the non-relativistic CFT do indeed contain all the relevant information about fields in the bulk of Lifshitz and other ‘non-relativistic’ space-times. However, full locality in the transverse direction cannot be achieved using smearing functions only, due to the presence of modes with vanishing boundary imprint. If and how the missing local bulk information can be extracted from the field theory remains an interesting open question. One possibility that comes to mind is to make use of non-local operators in the field theory, such as Wilson-loops [52]. At the very least, our analysis demonstrates that some parts of the holographic dictionary for nonrelativistic gauge/gravity dualities are more intricate than in the well-understood AdS/CFT case.

Acknowledgments

The authors would like to thank Tomas Andrade, Sheer El-Showk, Blaise Gouteraux, Monica Guica, Peter Koroteev, Leo Pando Zayas, Ioannis Papadimitriou, Simon Ross and Benson Way for fruitful discussions. CAK also thanks the Centro de Ciencias de Benasque Pedro Pascual for its hospitality during the July 2013 Gravity Workshop. This work was supported in part by the US Department of Energy under grant DE-SC0007859.

A WKB approximation

Our proof that smearing functions do not exist in Lifshitz and various other nonrelativistic spacetimes relies heavily on the use of WKB methods. While this approach in general only leads to approximate solutions, it is nevertheless able to capture the important qualitative behavior of the wavefunction that is needed in our analysis, up to a finite error. It is therefore crucial to discuss this method, as well as its limitations, in some detail.

We would like to find approximate solutions to equations of the form

$$\psi'' + \Omega^2(\zeta)\psi = 0, \quad (\text{A.1})$$

with $\Omega^2 > 0$ as $\zeta \rightarrow \infty$ and $\Omega^2 \sim -\zeta^{-2}$ as $\zeta \rightarrow 0$. Furthermore, we shall assume that for a given energy, there exists only one classical turning point with $\Omega^2(\zeta_0) = 0$. To capture all of these properties explicitly, we may write

$$\Omega^2 = K^2 - \frac{1}{\zeta^2} \left(\nu^2 - \frac{1}{4} + \mu(\zeta) \right), \quad (\text{A.2})$$

with $\lim_{\zeta \rightarrow 0} \mu(\zeta) = 0$ and $\nu > 1/2$. Notice that for $\nu \leq 1/2$ the qualitative picture would change considerably: The wavefunction becomes oscillating again close to the boundary, which requires a different treatment. For Lifshitz spacetime, we have $K = 1$ and $\mu = \alpha\zeta^{2-k}$, where $\zeta \equiv Ex$ (see (3.14)). We now make the standard WKB-ansatz

$$\psi \sim \frac{1}{\sqrt{P(\zeta)}} e^{i \int d\zeta' P(\zeta')}. \quad (\text{A.3})$$

Plugging into (A.1), we arrive at a differential equation for $P(\zeta)$:

$$P^2 - \Omega^2 + \frac{1}{2} \frac{P''}{P} - \frac{3}{4} \left(\frac{P'}{P} \right)^2 = 0. \quad (\text{A.4})$$

This equation can be solved perturbatively, assuming that the frequency Ω^2 is slowly-varying:

$$P^2 = Q_0 + \epsilon Q_1 + \epsilon^2 Q_2 + \dots, \quad (\text{A.5})$$

where

$$\begin{aligned} Q_0 &\equiv \Omega^2, \\ Q_1 &\equiv \frac{3}{4} \left(\frac{\Omega'}{\Omega} \right)^2 - \frac{1}{2} \frac{\Omega''}{\Omega}, \\ &\dots, \end{aligned} \quad (\text{A.6})$$

and we introduced an explicit parameter ϵ that counts the number of derivatives and needs to be set to 1 at the end. To lowest order, $P^2 \approx \Omega^2$ and the error can be estimated by comparing

the size of the first order to the zeroth order term. Away from the classical turning point ζ_0 , the full solution can be written as:

$$\psi(\zeta) = \begin{cases} (-\Omega^2)^{-\frac{1}{4}} \left[C e^{-\int_{\zeta_0}^{\zeta} d\zeta' \sqrt{-\Omega^2}} + D e^{\int_{\zeta_0}^{\zeta} d\zeta' \sqrt{-\Omega^2}} \right], & \zeta < \zeta_0; \\ (\Omega^2)^{-\frac{1}{4}} \left[a e^{i \int_{\zeta_0}^{\zeta} d\zeta' \sqrt{\Omega^2}} + b e^{-i \int_{\zeta_0}^{\zeta} d\zeta' \sqrt{\Omega^2}} \right], & \zeta > \zeta_0. \end{cases} \quad (\text{A.7})$$

As is obvious from (A.6), the WKB approximation always breaks down near the turning point. As usual, this can be dealt with by approximating the potential in the region close to ζ_0 by a linear function

$$\Omega^2 \approx \beta (\zeta - \zeta_0), \quad \beta \equiv \frac{d\Omega^2}{d\zeta}(\zeta_0) > 0. \quad (\text{A.8})$$

In this region, the solution is then given in terms of the Airy functions:

$$\psi_0 \approx E_1 \text{Ai} \left(\beta^{\frac{1}{3}} (\zeta_0 - \zeta) \right) + E_2 \text{Bi} \left(\beta^{\frac{1}{3}} (\zeta_0 - \zeta) \right). \quad (\text{A.9})$$

It has the following asymptotics:

$$\psi_0 \approx \begin{cases} \frac{(\zeta_0 - \zeta)^{-\frac{1}{4}}}{2\beta^{\frac{1}{12}} \sqrt{\pi}} \left[E_1 e^{-\frac{2}{3} \sqrt{\beta} (\zeta_0 - \zeta)^{\frac{3}{2}}} + 2E_2 e^{\frac{2}{3} \sqrt{\beta} (\zeta_0 - \zeta)^{\frac{3}{2}}} \right], & \zeta \ll \zeta_0; \\ \frac{(\zeta - \zeta_0)^{-\frac{1}{4}}}{2\beta^{\frac{1}{12}} \sqrt{\pi}} \left[(E_2 - iE_1) e^{i \left(\frac{\pi}{4} + \frac{2}{3} \sqrt{\beta} (\zeta - \zeta_0)^{\frac{3}{2}} \right)} + (E_2 + iE_1) e^{-i \left(\frac{\pi}{4} + \frac{2}{3} \sqrt{\beta} (\zeta - \zeta_0)^{\frac{3}{2}} \right)} \right], & \zeta \gg \zeta_0. \end{cases} \quad (\text{A.10})$$

On the other hand, for ζ close to, but not too close to ζ_0 , the exponent in (A.7) can be written as

$$\int_{\zeta_0}^{\zeta} d\zeta' \sqrt{|\Omega^2|} \approx \begin{cases} -\frac{2}{3} \sqrt{\beta} (\zeta_0 - \zeta)^{\frac{3}{2}}, & \zeta < \zeta_0; \\ \frac{2}{3} \sqrt{\beta} (\zeta - \zeta_0)^{\frac{3}{2}}, & \zeta > \zeta_0. \end{cases} \quad (\text{A.11})$$

Matching (A.10) and (A.7), we find

$$\begin{aligned} C &= \left(e^{-i\frac{\pi}{4}} a + e^{i\frac{\pi}{4}} b \right), \\ D &= \frac{i}{2} \left(e^{-i\frac{\pi}{4}} a - e^{i\frac{\pi}{4}} b \right). \end{aligned} \quad (\text{A.12})$$

Near the boundary ($\zeta \ll 1$), we then have

$$\psi(\zeta) = \frac{\zeta^{\frac{1}{2}}}{\left(\nu^2 - \frac{1}{4} \right)^{\frac{1}{4}}} \left(C e^{S_0(\zeta)} + D e^{-S_0(\zeta)} \right), \quad (\text{A.13})$$

where

$$S_0(\zeta) \equiv \int_{\zeta}^{\zeta_0} d\zeta' \sqrt{-\Omega^2}. \quad (\text{A.14})$$

Hence the solution near the boundary is determined entirely in terms of S_0 , which is given as an integral over the effective potential.

As a check of the validity of the WKB approximation, let us determine whether Q_1 in (A.5) remains small compared to Q_0 for all ζ . Consider the slightly more general case where $\Omega^2 \sim -\zeta^{-s}$ as $\zeta \rightarrow 0$. We find

$$Q_1 = -\frac{s(s-4)}{16\zeta^2}. \quad (\text{A.15})$$

For $s \neq 0, 4$, this term blows up near the boundary. For $s < 2$, it blows up faster than $Q_0 = \Omega^2$ itself, thus rendering the WKB approximation invalid. For $s > 2$, it blows up slower than Ω^2 , so the relative error approaches zero and we should expect WKB to yield accurate results. In the borderline case $s = 2$, which is the one that is interesting for us, the first order correction is in general comparable to the zero-th order term. Hence the lowest order approximation will a priori not give very accurate results.

Stated differently, for $s = 2$ the perturbative expansion (A.5) of P is not consistent, since in general the order n and order $n + 1$ terms will mix. To avoid this mixing, we need to find a way to explicitly move the $-1/(4\zeta^2)$ to one lower order in the expansion. Obviously, we could just declare

$$P^2 = \Omega^2 - \frac{1}{4\zeta^2} + O(\epsilon). \quad (\text{A.16})$$

This is equivalent to making the somewhat ad-hoc substitution $\nu^2 \rightarrow \nu^2 + 1/4$ in (A.5). A more rigorous way is to perform the following change of variables:

$$\begin{aligned} \zeta &\equiv e^w, \\ \psi &\equiv e^{\frac{w}{2}} u. \end{aligned} \quad (\text{A.17})$$

Then the Schrödinger equation reads

$$u'' + \omega^2 u = 0, \quad (\text{A.18})$$

where

$$\omega^2 \equiv e^{2w} - \nu^2 - \mu(w). \quad (\text{A.19})$$

It is easy to see that in these coordinates, the effective frequency is indeed slowly varying both in the deep UV and the deep IR. In fact, one can check that the first order term Q_1 becomes much smaller than Ω^2 in both limits. We see that in the new variables (A.17), the expansion (A.5) is consistent and the WKB solution is a good approximation everywhere, except in the vicinity of the turning point.

Repeating the steps (A.7) to (A.13) for (A.18) and changing back to our previous variables we arrive at

$$\psi = \left(\frac{\zeta}{\nu}\right)^{\frac{1}{2}} \left(C e^{S(\zeta)} + D e^{-S(\zeta)} \right), \quad (\text{A.20})$$

with

$$S(\zeta) \equiv \int_{\zeta}^{\zeta_0} d\zeta' \sqrt{-\Omega^2 + \frac{1}{4\zeta'^2}}. \quad (\text{A.21})$$

Not surprisingly, the effect of the coordinate transformation (A.17) is indeed to add an effective potential $\Delta U = 1/(4\zeta^2)$ to (A.2). Therefore, all we need to do in practice is to replace $\nu^2 \rightarrow \nu^2 + 1/4$. Let us emphasize that (A.18) is in fact equivalent to (A.1), so this substitution is now on a rigorous footing.

A.1 Example: AdS ($z = 1$)

For AdS, $z = 1$ and we have

$$\Omega^2 = 1 - \frac{\nu^2 - \frac{1}{4}}{\zeta^2}, \quad (\text{A.22})$$

where

$$\zeta = \sqrt{E^2 - p^2} \rho. \quad (\text{A.23})$$

Computing the integral (A.21), we find

$$S(\zeta) = -\sqrt{\nu^2 - \zeta^2} - \frac{\nu}{2} \log \left(\frac{\nu - \sqrt{\nu^2 - \zeta^2}}{\nu + \sqrt{\nu^2 - \zeta^2}} \right). \quad (\text{A.24})$$

Near the boundary ($\zeta \ll \nu$),

$$e^S \approx \left(\frac{e}{2\nu} \right)^{-\nu} \zeta^\nu. \quad (\text{A.25})$$

Plugging this result into (A.20) and rescaling back to the original field ϕ we arrive at the familiar-looking result

$$\phi(x) = A\rho^{d-\Delta} + B\rho^\Delta, \quad (\text{A.26})$$

where $\Delta \equiv (d+1)/2 + \nu$, and

$$\begin{aligned} A &= C e^{-\nu} 2^\nu \nu^{\nu-\frac{1}{2}} (E^2 - p^2)^{\frac{1}{4}-\frac{\nu}{2}}, \\ B &= i D e^\nu 2^{-\nu-1} \nu^{-\nu-\frac{1}{2}} (E^2 - p^2)^{\frac{1}{4}+\frac{\nu}{2}}. \end{aligned} \quad (\text{A.27})$$

Notice that the inclusion of the correction term ΔU was crucial to obtain the correct boundary behavior.

A.2 Example: $z = 2$ Lifshitz

For Lifshitz with $z = 2$, we have

$$\Omega^2 = 1 - \frac{\nu^2 - \frac{1}{4}}{\zeta^2} - \frac{\alpha}{\zeta}. \quad (\text{A.28})$$

The classical turning point is at

$$\zeta_0 = \frac{\alpha}{2} \left(1 + \sqrt{1 + \left(\frac{2\nu}{\alpha} \right)^2} \right). \quad (\text{A.29})$$

In this case, the WKB integral (A.21) can be evaluated to give

$$S = -\sqrt{\nu^2 + \alpha\zeta - \zeta^2} - \nu \log \left(\frac{\zeta (2\nu^2 + \alpha\zeta_0)}{\zeta_0 (2\nu^2 + \alpha\zeta + 2\nu\sqrt{\nu^2 + \alpha\zeta - \zeta^2})} \right) + \frac{\pi\alpha}{4} + \frac{\alpha}{2} \arcsin \left(\frac{\alpha - 2\zeta}{\sqrt{4\nu^2 + \alpha^2}} \right). \quad (\text{A.30})$$

In the near-boundary limit $\zeta/\nu \rightarrow 0$, with α/ν held fixed, we find

$$e^S \approx \left(\frac{\sqrt{\alpha^2 + (2\nu)^2}}{(2\nu)^2} \right)^{-\nu} \exp \left[-\nu + \frac{\alpha}{2} \left(\pi - \arctan \left(\frac{2\nu}{\alpha} \right) \right) \right] \cdot \zeta^{-\nu}. \quad (\text{A.31})$$

For $\alpha/\nu \ll 1$ this can be approximated as

$$e^S \approx \left(\frac{e}{2\nu} \right)^{-\nu} \zeta^{-\nu}, \quad (\text{A.32})$$

which is exactly what we found in the AdS case.

Hence high energy/low momentum modes do not “feel” the Lifshitz background, but instead behave like they would in the AdS case. Those are precisely the “free modes”, defined in section 3.1, which only have to tunnel through the ρ^{-2} -part of the potential. Notice that for finite momenta, the definitions of ζ in AdS (A.23) and Lifshitz (3.13) differ slightly. They do however agree in the $\alpha \rightarrow 0$ limit.

We are interested in the normalizable mode, which may be obtained by setting $C = 0$; this furthermore implies $D = e^{-i\frac{\pi}{4}}b$. Using (A.20), we see that

$$\left. \frac{|B|}{|b|} \right|_{\text{WKB}} = \frac{e^\nu}{\sqrt{\nu}(2\nu)^{2\nu}} (\alpha^2 + 4\nu^2)^{\nu/2} \exp \left[-\frac{\alpha}{2} \left(\pi - \arctan \left(\frac{2\nu}{\alpha} \right) \right) \right]. \quad (\text{A.33})$$

This may be compared with the exact $z = 2$ solution (3.29)

$$\frac{|B|}{|b|} = 2^{\frac{1}{2}+\nu} \frac{|\Gamma(\frac{1}{2} + \nu + i\frac{\alpha}{2})|}{\Gamma(1 + 2\nu)} e^{-\pi\alpha/4}. \quad (\text{A.34})$$

As an example, we show the behavior of the WKB and exact solution as a function of α for $\nu = 1$ in Figure 4.

It is straightforward to examine the behavior of the WKB and exact solutions in the small and large α limits. The $\alpha/\nu \ll 1$ limit was already considered above. In the opposite limit $\alpha/\nu \gg 1$, we find instead

$$e^S \approx \left(\frac{e}{2\nu} \right)^{-2\nu} \alpha^{-\nu} e^{\frac{\alpha\pi}{2}} \zeta^{-\nu}. \quad (\text{A.35})$$

Thus we obtain

$$\left. \frac{|B|}{|b|} \right|_{\text{WKB}} \approx \begin{cases} \left(\frac{e}{2} \right)^\nu \nu^{-(\nu+\frac{1}{2})}, & \text{for } \frac{\alpha}{\nu} \ll 1; \\ \frac{e^{2\nu}}{\sqrt{\nu}(2\nu)^{2\nu}} \alpha^\nu e^{-\frac{\pi\alpha}{2}}, & \text{for } \frac{\alpha}{\nu} \gg 1. \end{cases} \quad (\text{A.36})$$

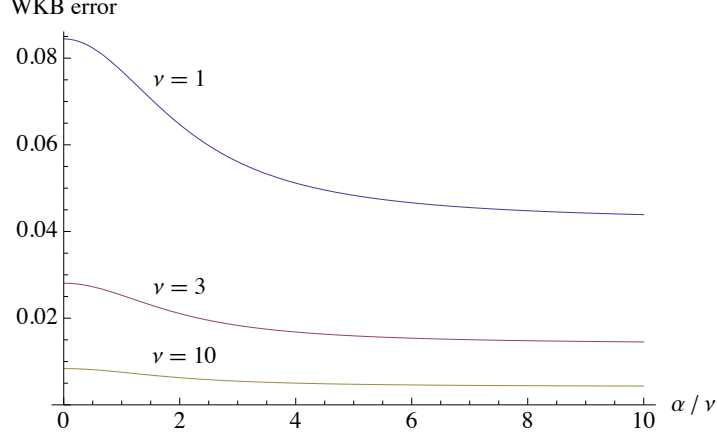


Figure 13. Comparison of the WKB amplitude factor with the exact result for $z = 2$ and $\nu = 1, 3$ and 10. The fractional WKB error is given by $(\eta_{\text{WKB}} - \eta_{\text{exact}})/\eta_{\text{exact}}$, where $\eta = |B|/|b|$.

This may be compared with the exact solution in the same limits

$$\frac{|B|}{|b|} \approx \begin{cases} \frac{2^{\nu+\frac{1}{2}} \Gamma(\frac{1}{2}+\nu)}{\Gamma(1+2\nu)}, & \text{for } \frac{\alpha}{\nu} \ll 1; \\ \frac{\sqrt{4\pi}}{\Gamma(1+2\nu)} \alpha^\nu e^{-\frac{\pi\alpha}{2}}, & \text{for } \frac{\alpha}{\nu} \gg 1. \end{cases} \quad (\text{A.37})$$

This demonstrates that the WKB solution gives the correct α behavior for both small and large α . Note that the ν dependent prefactors are different for finite ν , although they coincide in the large ν limit. This can be seen in Figure 13, where we plot the fractional difference between the WKB result and the exact solution for several values of ν . In particular, while the asymptotic behavior $|B|/|b| \sim \alpha^\nu e^{-\pi\alpha/2}$ is reproduced as $\alpha/\nu \rightarrow \infty$, the fractional error approaches a constant for fixed ν

$$\frac{\delta(|B|/|b|)}{|B|/|b|} \rightarrow \frac{\Gamma(1+2\nu)e^{2\nu}}{\sqrt{4\pi\nu}(2\nu)^{2\nu}} - 1 = \frac{1}{24\nu} + \frac{1}{1152\nu^2} + \dots \quad (\text{A.38})$$

One should keep in mind, however, that this will not affect our results on the absence of smearing functions for the Lifshitz background, as what is important is the exponential suppression near the boundary, and not the exact form of the prefactor.

Additionally, we did not need to know the exact relationship between the coefficient C in (A.20) and the non-normalizable mode A ; we only needed to know that setting $C = 0$ forces $A = 0$. In fact, the WKB approximation cannot pick out more about the relationship between A and C ; it cannot see if there is any of the normalizable mode B present in C as well. If we wanted to find the Green's function, we would have trouble. The Green's function is the response of the normalizable boundary mode to sourcing by the non-normalizable boundary mode, under infalling boundary conditions at the horizon; that is, $G = B/A|_{b=0}$. For the exact $z = 2$ solution, we find

$$\left. \frac{B}{A} \right|_{b=0} = (2i)^{2\nu} e^{2\pi i \nu} \frac{\Gamma(-2\nu)}{\Gamma(2\nu)} \frac{\Gamma(\frac{1}{2} + \nu + \frac{i\alpha}{2})}{\Gamma(\frac{1}{2} - \nu + \frac{i\alpha}{2})}. \quad (\text{A.39})$$

If we assume that the WKB term with coefficient C contributes only to the non-normalizable mode with coefficient A , then from WKB we would find, in the large α limit,

$$\left. \frac{|B|}{|A|} \right|_{\text{WKB}} = \left(\frac{e}{2\nu} \right)^{4\nu} \frac{\alpha^{2\nu}}{2} e^{-\alpha\pi}. \quad (\text{A.40})$$

These two expressions do not match, even when we are in a limit where the WKB error (see section (A.4)) is small. This mismatch, however, will not affect our analysis, because we only care about the case when the non-normalizable mode is completely turned off.

A.3 General Lifshitz

For the general Lifshitz case, we consider the effective potential

$$\Omega^2 = 1 - \frac{\nu^2}{\zeta^2} - \frac{\alpha}{\zeta^k}, \quad (\text{A.41})$$

where we recall that k is related to the critical exponent by $k = 2(1 - 1/z)$. We restrict to the case $z > 1$, corresponding to $0 < k < 2$. While the exact WKB integral may be performed numerically, it is in fact possible to extract the asymptotic behavior in the large α limit.

More precisely, we note that Ω^2 introduces several scales for ζ , depending on the relative importance of the three terms. In the UV, as $\zeta \rightarrow 0$, the ν^2/ζ^2 term will dominate, while in the IR, as $\zeta \rightarrow \infty$, the constant term will dominate. If $\alpha < \nu^k$, then the α/ζ^k term is not important. In this case, the $1/\zeta^2$ piece of the potential leads to power law behavior in the UV, but no exponential suppression in the wavefunction. On the other hand, for $\alpha > \nu^k$, an intermediate region $(\nu^2/\alpha)^{1/(2-k)} < \zeta < \alpha^{1/k}$ opens up, where the α/ζ^k term leads to tunneling behavior.

For $\alpha \gg \nu^k$, the UV and IR regions are well separated, and we may approximate the WKB integral according to

$$S = \int_{\zeta}^{\zeta_0} d\zeta' \sqrt{\frac{\nu^2}{\zeta'^2} + \frac{\alpha}{\zeta'^k} - 1} \approx \int_{\zeta}^{\zeta_*} d\zeta' \sqrt{\frac{\nu^2}{\zeta'^2} + \frac{\alpha}{\zeta'^k}} + \int_{\zeta_*}^{\zeta_0} d\zeta' \sqrt{\frac{\alpha}{\zeta'^k} - 1} = S_1 + S_2, \quad (\text{A.42})$$

where $(\nu^2/\alpha)^{1/(2-k)} \ll \zeta_* \ll \alpha^{1/k}$. The first integral may be performed by making the change of variables $u = (\alpha/\nu^2)\zeta^{2-k}$. The result is

$$S_1 = \frac{\nu}{2-k} \left[2\sqrt{1+u} + \log \frac{\sqrt{1+u}-1}{\sqrt{1+u}+1} \right] \Big|_{(\alpha/\nu^2)\zeta^{2-k}}^{(\alpha/\nu^2)\zeta_*^{2-k}}. \quad (\text{A.43})$$

Expanding for the lower limit near zero and the upper limit near infinity gives

$$S_1 = \frac{\nu}{2-k} \log \left(\frac{4\nu^2}{\alpha e^2} \right) - \nu \log \zeta + \frac{2\sqrt{\alpha}}{2-k} \zeta_*^{1-k/2} \left(1 - \frac{\nu^2}{2\alpha\zeta_*^{2-k}} + \dots \right). \quad (\text{A.44})$$

This gives the correct near-boundary behavior

$$\psi_{\text{WKB}} \sim \zeta^{1/2} e^{-S} \sim \zeta^{\nu+1/2}. \quad (\text{A.45})$$

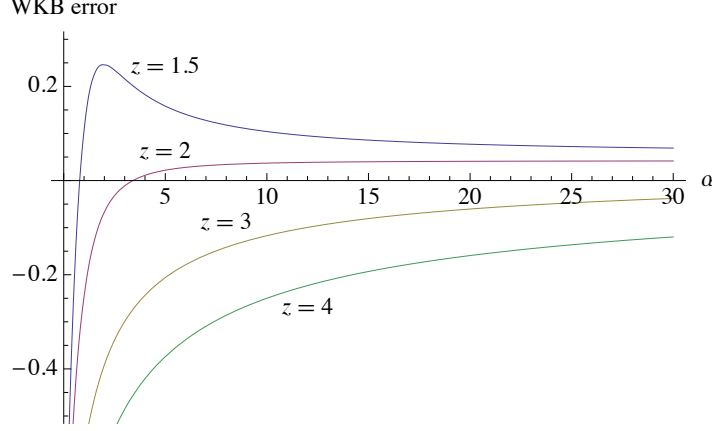


Figure 14. Comparison of the asymptotic WKB amplitude factor with the exact (numerical) result for $\nu = 1$, and $z = 1.5, 2, 3$ and 4 . The fractional WKB error is given by $(\eta_{\text{WKB}} - \eta_{\text{exact}})/\eta_{\text{exact}}$, where $\eta = |B|/|b|$. Note that the asymptotic WKB result (A.48) is only valid in the large α limit. The fractional error approaches a constant (dependent on ν) as $\alpha \rightarrow \infty$.

For the second integral, we let $u = \alpha/\zeta^k$, so that

$$S_2 = \frac{\alpha^{1/k}}{k} \int_1^{\alpha/\zeta_*^k} u^{-1-1/k} \sqrt{u-1} du. \quad (\text{A.46})$$

Although this integral can be expressed in terms of the incomplete Beta function, we only need the expansion for large α/ζ_*^k . The result is

$$S_2 = \frac{\sqrt{\pi}\Gamma(1/k - 1/2)}{2\Gamma(1/k)} \alpha^{1/k} - \frac{2\sqrt{\alpha}}{2-k} \zeta_*^{1-k/2} \left(1 - \frac{2-k}{2(2+k)} \frac{\zeta_*^k}{\alpha} - \dots \right). \quad (\text{A.47})$$

When S_1 and S_2 are added together, the leading terms in ζ_* cancel, while the rest vanish in the asymptotic limit. We thus obtain

$$\psi_{\text{WKB}} \sim \sqrt{\frac{\zeta}{\nu}} e^{-S} \sim \zeta^{\nu+1/2} \frac{1}{\sqrt{\nu}} \left(\frac{\alpha e^2}{4\nu^2} \right)^{\nu/(2-k)} \exp \left(-\frac{\sqrt{\pi}\Gamma(1/k - 1/2)}{2\Gamma(1/k)} \alpha^{1/k} \right). \quad (\text{A.48})$$

This agrees with (A.35) for $k = 1$, corresponding to $z = 2$. We have confirmed numerically that this WKB result for $\alpha \gg \nu^k$ reproduces the correct asymptotic behavior in α . As an example, we show the fractional error for several values of z at fixed $\nu = 1$ in Figure 14. As in the $z = 2$ case discussed above, for fixed ν , the exact prefactor is not reproduced by WKB. However, the exponential suppression is confirmed.

A.4 Error analysis

In addition to the explicit numerical analysis of the previous section, we would like to investigate the domain of validity of the WKB approximation analytically. In particular, this allows us to identify potentially problematic regions that yield a large error when integrated over, and identify when and where the WKB approximation breaks down.

In the coordinates (A.17), the effective frequency is given by

$$\omega^2 = e^{2w} - \alpha e^{(2-k)w} - \nu^2. \quad (\text{A.49})$$

The relative error can be estimated by

$$\begin{aligned} \frac{Q_1}{Q_0} = \frac{1}{\omega^6} & \left[\frac{1}{4} e^{4w} + \nu^2 e^{2w} + \frac{1}{16} \alpha^2 (2-k)^2 e^{2(2-k)w} \right. \\ & \left. + \frac{1}{4} \alpha (k^2 + k - 2) e^{(4-k)w} - \frac{1}{4} \nu^2 \alpha (2-k)^2 e^{(2-k)w} \right]. \end{aligned} \quad (\text{A.50})$$

Clearly, $Q_1/Q_0 \rightarrow 0$ as $w \rightarrow -\infty$, so the WKB approximation is always valid in the deep UV. The matching procedure near the turning point is only valid if there is some finite overlap between the matching region, where ω^2 is approximately linear, and the semiclassical region, where $|Q_1|/|Q_0| \ll 1$. Let us consider two separate cases:

1. $\alpha \ll \nu$: We can write $\omega^2 \approx e^{2w} - \nu^2$. The condition for the potential to be approximately linear is

$$\frac{(\omega^2)''(w_0)}{(\omega^2)'(w_0)} (w - w_0) \ll 1. \quad (\text{A.51})$$

Since the left hand side is of order $|w - w_0|$, the matching region is approximately given by $e^w \in [\nu e^{-1}, \nu e]$. To check if there is some overlap of this interval with the semiclassical region, let us plug the upper and lower bound into our error estimate:

$$\frac{|Q_1|}{|Q_0|} \approx \begin{cases} \frac{0.08}{\nu^2}, & e^w = \nu e^{-1}; \\ \frac{0.21}{\nu^2}, & e^w = \nu e. \end{cases} \quad (\text{A.52})$$

We see that for small ν (more precisely, for $\nu \lesssim 1/2$), the error becomes of order one and there is no overlap between the matching region and the semiclassical region. In this case, the matching procedure fails.

2. $\alpha \gg \nu$: We can write $\omega^2 \approx e^{2w} - \alpha e^{(2-k)w}$ for w near the turning point at $e^{w_0} \approx \alpha^{1/k}$. The condition (A.51) now gives $e^w \in [\alpha^{1/k} e^{-1}, \alpha^{1/k} e]$ and the error at the boundary points is $Q_1/Q_0 \sim \alpha^{-2/k} \cdot \text{const}$. Hence for α large enough the matching always yields good results.

Even though for large α the matching procedure works for all ν , one needs to be more careful: As we have seen previously, there are three different regimes of ζ , corresponding to each of the three terms in (A.49) dominating. In the region where $\alpha e^{(2-k)w}$ dominates, the relative error grows as w decreases (see (A.15)). If $\nu = 0$, the error continues to grow to infinity as we approach the boundary. However, for $\nu \neq 0$, the ν^2/ρ^2 part of the potential takes over at $\alpha e^{(2-k)w} \sim \nu^2$, and the relative error decreases again. Hence there is a local maximum of order

$$\frac{|Q_1|}{|Q_0|} \approx \frac{3}{32\nu^2}. \quad (\text{A.53})$$

For small ν , the WKB approximation breaks down in this region. We speculate that since $\alpha e^{(2-k)w} \sim \nu^2$ is precisely where the potential changes from p^2/ρ to ν^2/ρ^2 behavior, there is some nontrivial mixing between growing and decaying modes that the WKB approximation cannot account for. This mixing is stronger for small ν , as the difference between the relevant exponents, $\Delta_+ - \Delta_- = 2z\nu$, becomes small. Nevertheless, we can conclude that our WKB approximation can be trusted as long as $\nu \gtrsim 1/2$. Most importantly, the approximation becomes more and more accurate at large α/ν , which is precisely the regime we are interested in.

References

- [1] S. A. Hartnoll, *Lectures on holographic methods for condensed matter physics*, Class. Quant. Grav. **26**, 224002 (2009) [arXiv:0903.3246 [hep-th]].
- [2] J. McGreevy, *Holographic duality with a view toward many-body physics*, Adv. High Energy Phys. **2010**, 723105 (2010) [arXiv:0909.0518 [hep-th]].
- [3] L. Huijse and S. Sachdev, *Fermi surfaces and gauge-gravity duality*, Phys. Rev. D **84**, 026001 (2011) [arXiv:1104.5022 [hep-th]].
- [4] S. Sachdev, *Condensed Matter and AdS/CFT*, Lect. Notes Phys. **828**, 273 (2011) [arXiv:1002.2947 [hep-th]].
- [5] S. F. Ross and O. Saremi, *Holographic stress tensor for non-relativistic theories*, JHEP **0909**, 009 (2009) [arXiv:0907.1846 [hep-th]].
- [6] S. F. Ross, *Holography for asymptotically locally Lifshitz spacetimes*, Class. Quant. Grav. **28**, 215019 (2011) [arXiv:1107.4451 [hep-th]].
- [7] I. Papadimitriou, *Holographic Renormalization of general dilaton-axion gravity*, JHEP **1108**, 119 (2011) [arXiv:1106.4826 [hep-th]].
- [8] M. Baggio, J. de Boer and K. Holsheimer, *Hamilton-Jacobi Renormalization for Lifshitz Spacetime*, JHEP **1201**, 058 (2012) [arXiv:1107.5562 [hep-th]].
- [9] I. Papadimitriou, *Holographic renormalization as a canonical transformation*, JHEP **1011**, 014 (2010) [arXiv:1007.4592 [hep-th]].
- [10] R. B. Mann and R. McNees, *Holographic Renormalization for Asymptotically Lifshitz Spacetimes*, JHEP **1110**, 129 (2011) [arXiv:1107.5792 [hep-th]].
- [11] W. Chemissany, D. Geissbuhler, J. Hartong and B. Rollier, *Holographic Renormalization for z=2 Lifshitz Space-Times from AdS*, Class. Quant. Grav. **29**, 235017 (2012) [arXiv:1205.5777 [hep-th]].
- [12] D. Anninos, W. Li, M. Padi, W. Song and A. Strominger, *Warped AdS₃ Black Holes*, JHEP **0903**, 130 (2009) [arXiv:0807.3040 [hep-th]].
- [13] S. K. Chakrabarti, P. R. Giri and K. S. Gupta, *Scalar field dynamics in warped AdS₃ black hole background*, Phys. Lett. B **680**, 500 (2009) [arXiv:0903.1537 [hep-th]].
- [14] Y. Liu and Y. -W. Sun, *Consistent Boundary Conditions for New Massive Gravity in AdS₃*, JHEP **0905**, 039 (2009) [arXiv:0903.2933 [hep-th]].

- [15] D. Anninos, G. Compère, S. de Buyl, S. Detournay and M. Guica, *The Curious Case of Null Warped Space*, JHEP **1011**, 119 (2010) [arXiv:1005.4072 [hep-th]].
- [16] G. Compère, W. Song and A. Strominger, *New Boundary Conditions for AdS_3* , JHEP **1305**, 152 (2013) [arXiv:1303.2662 [hep-th]].
- [17] S. Kachru, X. Liu and M. Mulligan, *Gravity Duals of Lifshitz-Like Fixed Points*, Phys. Rev. D **78** (2008) 106005 [arXiv:0808.1725 [hep-th]].
- [18] H. Braviner, R. Gregory and S. F. Ross, *Flows involving Lifshitz solutions*, Class. Quant. Grav. **28**, 225028 (2011) [arXiv:1108.3067 [hep-th]].
- [19] H. Singh, *Holographic flows to IR Lifshitz spacetimes*, JHEP **1104**, 118 (2011) [arXiv:1011.6221 [hep-th]].
- [20] H. Singh, *Lifshitz to AdS flow with interpolating p -brane solutions*, JHEP **1308**, 097 (2013) [arXiv:1305.3784 [hep-th]].
- [21] S. Harrison, S. Kachru and H. Wang, *Resolving Lifshitz Horizons*, arXiv:1202.6635 [hep-th].
- [22] J. Bhattacharya, S. Cremonini and A. Sinkovics, *On the IR completion of geometries with hyperscaling violation*, JHEP **1302**, 147 (2013) [arXiv:1208.1752 [hep-th]].
- [23] G. Knodel and J. T. Liu, *Higher derivative corrections to Lifshitz backgrounds*, arXiv:1305.3279 [hep-th].
- [24] K. Goldstein, S. Kachru, S. Prakash and S. P. Trivedi, *Holography of Charged Dilaton Black Holes*, JHEP **1008**, 078 (2010) [arXiv:0911.3586 [hep-th]].
- [25] K. Narayan, *On Lifshitz scaling and hyperscaling violation in string theory*, Phys. Rev. D **85**, 106006 (2012) [arXiv:1202.5935 [hep-th]].
- [26] X. Dong, S. Harrison, S. Kachru, G. Torroba and H. Wang, *Aspects of holography for theories with hyperscaling violation*, JHEP **1206**, 041 (2012) [arXiv:1201.1905 [hep-th]].
- [27] P. Bueno, W. Chemissany, P. Meessen, T. Ortin and C. S. Shahbazi, *Lifshitz-like Solutions with Hyperscaling Violation in Ungauged Supergravity*, JHEP **1301**, 189 (2013) [arXiv:1209.4047 [hep-th]].
- [28] P. Dey and S. Roy, *From AdS to Schrödinger/Lifshitz dual space-times without or with hyperscaling violation*, arXiv:1306.1071 [hep-th].
- [29] M. Edalati, J. F. Pedraza and W. Tangarife Garcia, *Quantum Fluctuations in Holographic Theories with Hyperscaling Violation*, Phys. Rev. D **87**, no. 4, 046001 (2013) [arXiv:1210.6993 [hep-th]].
- [30] V. Balasubramanian, P. Kraus and A. E. Lawrence, *Bulk versus boundary dynamics in anti-de Sitter space-time*, Phys. Rev. D **59**, 046003 (1999) [hep-th/9805171].
- [31] V. Balasubramanian, P. Kraus, A. E. Lawrence and S. P. Trivedi, *Holographic probes of anti-de Sitter space-times*, Phys. Rev. D **59**, 104021 (1999) [hep-th/9808017].
- [32] I. Bena, *On the construction of local fields in the bulk of AdS_5 and other spaces*, Phys. Rev. D **62**, 066007 (2000) [hep-th/9905186].
- [33] A. Hamilton, D. N. Kabat, G. Lifshytz and D. A. Lowe, *Local bulk operators in AdS/CFT: A Boundary view of horizons and locality*, Phys. Rev. D **73**, 086003 (2006) [hep-th/0506118].

- [34] A. Hamilton, D. N. Kabat, G. Lifschytz and D. A. Lowe, *Holographic representation of local bulk operators*, Phys. Rev. D **74**, 066009 (2006) [hep-th/0606141].
- [35] V. Balasubramanian, S. B. Giddings and A. E. Lawrence, *What do CFTs tell us about Anti-de Sitter space-times?*, JHEP **9903**, 001 (1999) [hep-th/9902052].
- [36] T. Banks, M. R. Douglas, G. T. Horowitz and E. J. Martinec, *AdS dynamics from conformal field theory*, hep-th/9808016.
- [37] A. L. Fitzpatrick and J. Kaplan, *Scattering States in AdS/CFT*, arXiv:1104.2597 [hep-th].
- [38] R. Bousso, B. Freivogel, S. Leichenauer, V. Rosenhaus and C. Zukowski, *Null Geodesics, Local CFT Operators and AdS/CFT for Subregions*, arXiv:1209.4641 [hep-th].
- [39] S. Leichenauer and V. Rosenhaus, *AdS black holes, the bulk-boundary dictionary, and smearing functions*, Phys. Rev. D **88**, **026003** (2013) [arXiv:1304.6821 [hep-th]].
- [40] K. Copsey and R. Mann, *Pathologies in Asymptotically Lifshitz Spacetimes*, JHEP **1103**, 039 (2011) [arXiv:1011.3502 [hep-th]].
- [41] G. T. Horowitz and B. Way, *Lifshitz Singularities*, Phys. Rev. D **85**, 046008 (2012) [arXiv:1111.1243 [hep-th]].
- [42] C. Hoyos and P. Koroteev, *On the Null Energy Condition and Causality in Lifshitz Holography*, Phys. Rev. D **82**, 084002 (2010) [Erratum-ibid. D **82**, 109905 (2010)] [arXiv:1007.1428 [hep-th]].
- [43] J. T. Liu and Z. Zhao, *Holographic Lifshitz flows and the null energy condition*, arXiv:1206.1047 [hep-th].
- [44] N. Bao, X. Dong, S. Harrison and E. Silverstein, *The Benefits of Stress: Resolution of the Lifshitz Singularity*, Phys. Rev. D **86**, 106008 (2012) [arXiv:1207.0171 [hep-th]].
- [45] J. M. Maldacena, *The Large N limit of superconformal field theories and supergravity*, Adv. Theor. Math. Phys. **2**, 231 (1998) [hep-th/9711200].
- [46] S. S. Gubser, I. R. Klebanov and A. M. Polyakov, *Gauge theory correlators from noncritical string theory*, Phys. Lett. B **428**, 105 (1998) [hep-th/9802109].
- [47] E. Witten, *Anti-de Sitter space and holography*, Adv. Theor. Math. Phys. **2**, 253 (1998) [hep-th/9802150].
- [48] C. Keeler, *Scalar Boundary Conditions in Lifshitz Spacetimes*, arXiv:1212.1728 [hep-th].
- [49] T. Andrade and S. F. Ross, *Boundary conditions for scalars in Lifshitz*, Class. Quant. Grav. **30**, 065009 (2013) [arXiv:1212.2572 [hep-th]].
- [50] T. Andrade and S. F. Ross, *Boundary conditions for metric fluctuations in Lifshitz*, arXiv:1305.3539 [hep-th].
- [51] F. Brau and F. Calogero *Upper and lower limits for the number of S-wave bound states in an attractive potential*, J. Math. Phys. **44**, 1554 (2003).
- [52] L. Susskind and N. Toumbas, *Wilson loops as precursors*, Phys. Rev. D **61**, 044001 (2000) [hep-th/9909013].